A Population WB-PBPK Model of Colistin and its Prodrug CMS in Pigs: Focus on the Renal Distribution and Excretion

Alexis Viel, Jérôme Henri, Salim Bouchène, Julian Laroche, Jean-Guy Rolland, Jacqueline Manceau, Michel Laurentie, William Couet, Nicolas Grégoire

A population WB-PBPK model of colistin and its prodrug CMS in pigs: focus on the renal distribution and excretion.

Running head**:** WB-PBPK model for CMS and colistin in pigs

Alexis Viel[1,2,3], Jérôme Henri[2], Salim Bouchène[4], Julian Laroche[1,5], Jean-Guy Rolland[2], Jacqueline Manceau[2], Michel Laurentie[2], William Couet[1,3,5], Nicolas Grégoire[3]

1. INSERM, Unit 1070, Poitiers, France
2. Anses, Laboratoire de Fougères, Fougères, France
3. UFR Médecine-Pharmacie, Poitiers, France
4. Certara, Paris, France
5. CHU de Poitiers, Poitiers, France

Corresponding author:

Nicolas Grégoire

Tel.: +33 5 49 36 64 36.

E-mail address: nicolas.gregoire@univ-poitiers.fr

Abstract

Purpose: The objective was the development of a whole-body physiologically-based pharmacokinetic (WB-PBPK) model for colistin, and its prodrug colistimethate sodium (CMS), in pigs to explore their tissue distribution, especially in kidneys.

Methods: Plasma and tissue concentrations of CMS and colistin were measured after systemic administrations of different dosing regimens of CMS in pigs. The WB-PBPK model was developed based on these data according to a non-linear mixed effect approach and using NONMEM software. A detailed sub-model was implemented for kidneys to handle the complex disposition of CMS and colistin within this organ.

Results: The WB-PBPK model well captured the kinetic profiles of CMS and colistin in plasma. In kidneys, an accumulation and slow elimination of colistin were observed and well described by the model. Kidneys seemed to have a major role in the elimination processes, through tubular secretion of CMS and intracellular degradation of colistin. Lastly, to illustrate the usefulness of the PBPK model, an estimation of the withdrawal periods after veterinary use of CMS in pigs was made.

Conclusion: The WB-PBPK model gives an insight into the renal distribution and elimination of CMS and colistin in pigs; it may be further developed to explore the colistin induced-nephrotoxicity in humans.

Keywords: colistin; CMS; kidneys; PBPK model; pigs;

ABBREVIATIONS

ADME: Absorption, distribution, metabolism, excretion

BLOQ: below the limit of quantification

BW: body weight

CBA: colistin base activity

CMS: colistimethate sodium

DV: observed value

fu: unbound fraction

GFR: glomerular filtration rate

GIT: gastro-intestinal tract

HPLC-MS/MS: high-performance liquid chromatography coupled with tandem mass spectrometry

IIV: interindividual variability

IPRED: individual prediction

IV: intravenous

IM: intramuscular

LOQ: limit of quantification

MRL: maximal residue limits

NLME: nonlinear mixed effects

OFV: objective function value

PBPK: physiologically-based pharmacokinetic

PK: pharmacokinetics

PRED: population prediction

RV: residual variability

SIR: sampling importance resampling

$t_{1/2}$: half-life

VPC: visual predictive checks

WB-PBPK: whole body physiologically-based pharmacokinetic

WP: withdrawal period

INTRODUCTION

Colistin is an old peptide antibiotic from the polymyxin family that is used in human and veterinary medicines. In food producing animals, colistin is widely used as colistin sulphate to treat bacterial digestive infections. The use of its pro-drug, the colistimethate sodium (CMS), is the most frequent in human medicine but CMS can also be found as animal treatment. In human, in many cases colistin has become the last resort antibiotic against multi-resistant bacteria (1). Colistin is the active moiety and is formed from CMS hydrolysis within the body (2). CMS is a mixture of methanesulfonated molecules, which are hydrolysed in colistin by loss of methanesulfonate groups (3). The structures of colistin and CMS are responsible for their complex absorption, distribution, metabolism, and excretion (ADME), which depend on poorly described biological mechanisms (see below). Because of the renewed interest for colistin, clarifying this complexity is nevertheless essential in order to improve dosing adjustments and to avoid toxic effects (4).

Colistin and CMS have a high molecular weight (1167 g/mol and 1632 g/mol, respectively) and are ionized (cationic and anionic, respectively) at physiological pH (5), implying a weak passage of cellular membranes and physiological barriers. Hence, their distributions are supposed to be mainly within the extracellular spaces (6). According to few studies in animals, colistin is also suspected to bind to tissues (7, 8). Concerning elimination mechanisms, CMS is partially excreted unchanged in urine, as seen in healthy humans and rats (2, 6). Conversely, colistin excretion in urine is very low due to a major tubular reabsorption after glomerular filtration (2), and colistin tends to accumulate in kidney tissue (9, 10). Specifically, colistin mainly accumulates within cells of the proximal tubules (11), where this extensive reabsorption takes place (12, 13). This is an active process for which carrier-mediated uptakes involving different renal transporters, like PEPT2 (14) or megalin (10), have been identified. Moreover, an accumulation of polymyxins in intracellular organelles (like mitochondria and endoplasmic reticulum) has been shown (12) which could be linked to cellular death-pathways (15)

98 and nephrotoxic effects (15, 16). Colistin metabolism has not been described, but considering its
99 peptidic structure it probably involves hydrolysis mechanisms (1).

100 Thus, the disposition of CMS and colistin within kidneys is not fully understood but has great
101 implication in clinical practice, due to the dose-limiting nephrotoxicity. Classical pharmacokinetic
102 approaches could be used to describe plasma profiles of both compounds but are inefficient to handle
103 tissue concentrations. Moreover, it is quite difficult to collect experimental data in humans, especially
104 in tissues, for obvious ethical reasons. Physiologically-based pharmacokinetics (PBPK) modelling, based
105 on animal experiments, is a pertinent approach for this task. In addition to their ability to describe
106 tissue distributions, these models are useful to perform some extrapolations from animals to human
107 (17). A previous whole-body PBPK (WB-PBPK) model has been developed for CMS and colistin from rat
108 experiments (18). However, several assumptions were made, especially for the renal/urinary
109 distribution of CMS and colistin, without experimental data in tissue to support them. One advantage
110 of this PBPK model was the use of a non-linear mixed effect (NLME) modelling approach (19) in order
111 to handle inter-individual variabilities. Here, we refined this WB-PBPK model using numerous
112 experimental plasma, urinary and tissue data from pigs, with a special focus on kidney exposure to
113 colistin. Pigs were chosen for their physiological proximity to human (20), facilitating future inter-
114 specie extrapolations.

115 The description of colistin pharmacokinetics in whole body is also interesting in the veterinary
116 field. Indeed, for food safety concern, maximal residue limits (MRL) for colistin have been defined in
117 edible tissues originating from food producing animals (21), e.g. pigs. These MRLs ensure that
118 consumers can eat products from animals treated with colistin, without risk for their health. Therefore,
119 a period is necessary between the last administration and the production of foodstuffs in order that
120 colistin concentrations decrease below the MRL. This time is regulatory defined as the withdrawal
121 period (WP). Linear regression based-methods are traditionally used to estimate the WP (22).
122 However, the development of population PBPK modelling for this purpose in on going, due to their
123 ability to predict tissue concentrations (23).

The aim of this study was first the development of a population PBPK model in pigs for colistin and its prodrug, CMS, using a NMLE approach with a focus on the renal disposition of both compounds. As an application of this PBPK model, its predictive ability to describe plasma and tissue concentrations was then used for estimating withdrawal period of colistin in pigs, highlighting one of the advantages of this modelling approach.

MATERIALS AND METHODS

Chemicals

CMS (Colymicine 1 MIU; Sanofi Aventis, Paris, France) was used for all experiments. It was freshly reconstituted in 0.9% NaCl prior to each administration. To avoid any spontaneous hydrolysis of CMS into colistin, reconstituted CMS solutions were kept at +4°C and administered within the first hour after reconstitution.

Animals

Forty-six (46) crossbred female swine (Duroc × Landrace × Large white) were purchased from INRA (Le Rheu, France) with no history of polymyxin treatments. The animals were housed in collective pens and acclimatized for one week under standard farming conditions before the experiments. They were between 12 and 14 weeks old with a body weight (BW) ranging from 45 to 55 kg at the beginning of the experiments.

Then pigs were housed by groups of two for those receiving repeated intramuscular (IM) administrations. Pigs carrying a venous catheter were kept alone in metabolism cages for a maximum of 4 days.

Animal killing was performed with electronarcosis, that induced instantaneous insensibility, following by bleeding with aorta section.

All experiments were conducted in accordance with the local ethical comity and were registered under the references 2905-2015112717486085 and 6528-201608251410563.

In vivo experiments

- Catheter implantation

For pigs receiving at least one intravenous (IV) administration of CMS, central venous catheters were implanted. These animals were firstly sedated with an IM injection of ketamine at 20 mg/kg (Imalgène, Mérial, Lyon, France) and xylazine at 2 mg/kg (Rompun, Bayer, Loos, France). Then, they were intubated and kept anesthetized by inhalation with isoflurane 2.5% (IsoFlo, Zoetis, Malakoff, France) during all the surgical procedure. An incision was performed on the neck under local anaesthesia with xylocaine (Xylovet, CEVA, Libourne, France). After dilaceration of superficial tissues and muscles, two catheters were implanted in the jugular vein, one for drug administration and one for blood sampling. After surgery, pigs rested 48 h alone in their box. Then, they were housed separately in metabolism cage in order to facilitate drug administration and blood/urine sampling.

- Sampling

Blood sampling: for pigs harbouring a venous catheter, 1.5 mL of blood was taken at each sample. Catheter was then flushed with heparinised saline solution. Pigs without catheter were restrained by an operator using a snout rope while a second one was sampling blood with a vacuum tube from the external jugular vein. Immediately after sampling, plasma was chilled on ice bath, then separated by centrifugation (3000 g) at 4°C and kept in polypropylene tubes at -80°C until assay.

Urine sampling: spontaneous urination was gathered only from animals kept in metabolism cage; volume of urine was measured and then a 20 mL-sample was kept in polypropylene tubes at -80°C until assay.

Tissue sampling: each organ (except muscles, fat and skin) was entirely collected after killing, weighted and its volume measured by water displacement. A sample was taken from the area of the left gluteal muscle (including skin) for skin and muscles analysis. A piece of abdominal fat was taken for the adipose analysis. Then, tissues were cut into small pieces, rinsed with saline solution, put into polypropylene tubes and kept at -80°C until assay. Tissues were chilled within the first 30-min following the euthanasia of pigs. The possible hydrolysis of CMS during that period, and its impact on the estimations of partition coefficients (see experiment n°3 below), were considered as negligible.

- Experimental setup for PBPK model calibration

Different dosing regimens (doses and route of administration) of CMS were administered for model calibration (a brief description is given in Table I). Some pigs were used for several experiments (n°1, 2 and 3, see below): in that case the potential residual concentrations from previous administrations were considered for modelling.

Experiment N°1/Plasma and kidney PK after a single IV administration (10 pigs): a 1-h constant IV infusion of CMS at 125,000 UI/kg of BW (corresponding to 3.75 mg/kg CBA or 10 mg/kg of CMS base (24)) was administered via the central catheter. Blood samples (n=12 per pig) were taken from 0.5 h to 32 h after the start of CMS administration. Urine samples were collected over two intervals (0-8h and 8-24h after CMS administration) for 6 pigs, and for the remaining 4 animals between 6 and 9 successive urine samples were collected depending on technician availability. Four pigs were sacrificed at 32 h and their kidneys were immediately removed and processed as described in sampling section.

198 *Experiment N°2/Plasma PK after a single IM administration (6 pigs)*: CMS solution (125,000 UI/kg of
199 BW) was administered as two injections of about 10 mL into gluteal muscle of each side. Blood samples
200 (n=12 per pig) were taken from 0.25 h to 24 h after the injection.
201
202 *Experiment N°3/Tissue partition coefficients (6 pigs):* A dosing regimen was elaborated to achieve
203 steady state of CMS and colistin in order to estimate the tissue to plasma partition coefficients (Kp):
204 pigs were firstly infused during 1 h with a loading dose of CMS at 75,000 UI/kg; then a break of 1.5 h
205 was done to get sufficient *in vivo* hydrolysis of CMS into colistin; finally, 50,000 UI/kg of CMS was
206 administered as a 4 h-infusion. Blood samples were taken during the 4 h-infusion to assess steady-
207 state in plasma; at the end of the infusion pigs were sacrificed and their blood, lungs, brain, heart,
208 abdominal fat, skin, gluteal muscle, duodenum, liver and kidneys were immediately removed and
209 processed as described in sampling section.

210 *Experiment N°4/Plasma and kidney PK during and after repeated IM administrations (15 pigs)*:
211 repeated CMS administrations were performed to study colistin renal accumulation. Pigs were
212 randomly divided into 5 groups of 3 individuals. They received two IM injections of CMS per day at
213 25,000 UI/kg with a day-delay of 9 h (and 15 h during night). One group received 2 administrations (1
214 day) and were slaughtered 15 h after last injection; one group received 6 administrations (3 days) and
215 were slaughtered 15 h after last injection; last 3 groups received 14 administrations (7 days) and were
216 sequentially slaughtered at 15, 39 and 63 h after last injection. IM administrations were given on the
217 neck and on top of gluteal muscles with a side alternation at each injection. Blood samples were taken
218 during the treatment period in a sparse sampling way (between 1 and 3 per pig), each animal being
219 sampled every 48 h at most. At sacrifice, blood and kidneys were collected and processed as described
220 in sampling section.
221
222 • <u>Experimental setup for model validation</u>

Experiment N°5/Tissue and plasma PK after IM injections of CMS following the recommended veterinary dose (20 pigs): repeated CMS administrations were performed over 3 days with two IM injections per day at 25,000 UI/kg with a day-delay of 9 h (and 15 h during night). Then, pigs were sacrificed by groups of 4 at 1 h, 3 h, 5.5 h, 7.5 h, 15 h after last administration and their blood and fat, muscles, kidney, liver, skin (edible tissues) were collected as described above.

Determination of the unbound fraction (fu) of CMS in plasma

The plasma fu of colistin in pigs (40%) was obtained from the literature (25). As no value was retrieved for CMS in the literature, we determined $fu_{\_CMS}$ by ultrafiltration. Briefly, CMS was added to blank plasma from pig at a theoretical concentration of 5 µg/mL and 0.5 µg/mL, then ultra-filtrated through a cellulose-membrane (Centrifree, Merck, Alsace, France) by centrifugation (3000 g) at 37 °C during 30 min. A similar experiment was performed in buffer instead of plasma in order to take into account the loss due to CMS hydrolysis at 37 °C in plasma (3), and the potential non-specific binding of CMS to the lab material (5). All filtrates were kept at -20°C before assay (less than 1 week). All these experiments were realized in triplicates.

Analytical methods

Plasma and urinary CMS and colistin concentrations were assayed with a validated high performance liquid chromatography tandem mass spectrometry (HPLC-MS/MS) method using polymyxin B as internal standard, as described elsewhere (26). With this analytical method, CMS determination is achieved in an indirect way: a separate aliquot of each sample was pre-treated with sulphuric acid at 0.5M (for 1 h at room temperature) to hydrolyse CMS to colistin and the concentration of CMS was then determined by difference between the concentrations measured before and after the acid hydrolysis, accounting for the differences in molecular weights of CMS and colistin.

For tissues, this method was adapted. Briefly, standards and quality controls were prepared from blank tissues. A sample of 100 mg for each organ was taken and 980 µL of blank plasma was added

before homogenization with T-18 Ultra-Turrax homogenizer (KA®-Werke GmbH & Co. KG, Germany). Then 20 µL of a colistin solution (diluted in a 50/50 mix plasma/water) was added to obtain standard curves. After vortexing and centrifugation (4000 rpm for 10 min), supernatants were assayed as described for plasma (26). For samples, the same procedure was realized but 20 µL of a 50/50 mix plasma/water solution was added instead of 20 µL of colistin solution. Calibration range of colistin was from 0.020 µg/mL to 10 µg/mL in plasma and 0.2 to 100 µg/g In tissues; the concentrations of quality controls were at 0.16, 0.63 and 3.80 µg/mL in plasma and 0.5,5 and 75 µg/g in tissues; the limit of quantification were 0.02 µg/mL for colistin in plasma; 0.2 µg/g for colistin in all tissues. For CMS, the LOQ was 0.15 µg/mL in plasma and 1 µg/g in tissues.

For the assay in kidney, the intracellular localization of colistin made imprecise the discrimination between colistin and CMS concentrations. Indeed, the lysis of cells occurred both during the crushing phase and the acidic phase used for CMS determination. Therefore, the concentrations measured in kidneys corresponded to the sum of CMS and colistin, expressed as colistin.

Development of the PBPK model

- Model structure

The PBPK model was based on a previous published model developed from rats, using plasma and various tissue concentrations (18). It is composed of 9 compartments corresponding to the main body organs (lungs, heart, liver, fat, skin, gastro-intestinal tract, brain, muscles, and kidneys), two blood compartments (arterial and venous) and one excretion compartment (urine) (Fig. 1A). Remaining body was lumped into a compartment named “rest of body”. Volumes of compartments and blood flows were fixed to physiological values reported in the literature (25, 27-42). These values depended on individual bodyweights and cardiac output (which also depends on bodyweight), respectively (Table II). The cardiac output was corrected by the haematocrit to get the total plasma flow. Because molecular weights of CMS and colistin are small with respect to passage across endothelial walls, it

was expected that distribution within extracellular fluid was rapid (6) and a perfusion limited model was assumed for all organs except kidneys in which active intra-cellular transport occurs (see below).

Drug distribution in each tissue compartment (except kidney and bladder) was upon the dependency of Kps. CMS and colistin Kps were determined at the end of the perfusion established to reach the steady state for both drugs (experiment n°3) as follows (Eq. 1):

$$Kp = \frac{Ctis_{\_SS}}{Cplas_{\_SS}} \quad \text{(Eq. 1)}$$

where Kp is the partition coefficient of the tissue, $Ctis_{\_SS}$ is the concentration measured at steady-state in the overall tissue, i.e. containing both extracellular and intracellular spaces; $Cplas_{\_SS}$ is the plasma concentration of CMS or colistin at steady-state.

The hydrolysis of CMS into colistin was assumed to take place in every compartment (including plasma), with a common hydrolysis constant (K_{hyd_CMS}) (Fig. 1B). This assumption was supported by a previous experiment in rats, showing no significant differences of the hydrolysis rates between plasma and various tissue homogenates (18). This constant was estimated during model calibration. Thus, for each tissue an intrinsic hydrolysis clearance (CL_{hyd_CMS}) was expressed as follows (Eq. 2):

$$CL_{hyd\_CMS} = V_{tissue}.K_{hyd\_CMS} \quad \text{(Eq. 2)}$$

Where V_{tissue} is the volume of the corresponding tissue.

For colistin, the elimination occurs via mechanisms not yet described. Similar to CMS, an elimination process was defined based on a constant (K_{deg_COLI}) common to all the organs (Fig. 1B) and estimated during model calibration. The intrinsic degradation clearance (CL_{deg_COLI}) was defined as (Eq. 3):

$$CL_{deg\_COLI} = V_{tissue}.K_{deg\_COLI} \quad \text{(Eq. 3)}$$

Where V_{tissue} is the volume of the corresponding tissue.

Kidneys were divided into sub-compartments (Fig. 2) due to the particular distribution/elimination pathways of polymyxins within this organ. Renal vascular, extra-vascular and tubular intracellular spaces as well as luminal proximal tubular compartments were defined. CMS was eliminated in kidneys either by urine excretion or by hydrolysis into colistin. The latter one was assumed to take place in every sub-compartments of the kidney (according to a constant rate K_{hyd_CMS}). Concerning the urine excretion of unchanged CMS, it was due either to glomerular filtration or potentially to secretion of CMS from the extra-vascular space to the tubular lumen (through tubular cells), as outlined for rats in a previous study (2). Therefore, a glomerular filtration clearance (CL_{GFR_CMS}) was included in the structure of the base model, originating from kidney vascular space compartment and going into the proximal tubules one (43). CL_{GFR_CMS} was calculated as the product of the glomerular filtration rate (GFR) and the $fu_{\_CMS}$ in plasma (experimentally determined). The potential secretion of CMS was tested during model development.

Within kidney, colistin was also eliminated either by urine excretion or by metabolism (degradation). The urinary excretion corresponded to the colistin filtrated by the glomeruli (expressed by CL_{GFR_COLI}) that was neither metabolized nor reabsorbed within the tubules. Indeed, colistin undergoes major tubular reabsorption: it was observed that more than 90% of excreted colistin was reabsorbed in rats (9). Colistin is then mainly located in proximal tubular cells as shown with *in vitro* studies with polymyxins (11-13). Therefore, a reabsorption clearance of colistin (CL_{reabs_COLI}) was estimated in the model, originating from the tubular lumen into the intracellular sub-compartment. Colistin renal metabolism was assumed to take place in every sub-compartment (at constant rate corresponding to K_{deg_COLI}). Due to the lack of data and the kidney physiology that is close between human and pig (20), the flow in the proximal tubule (Qtub) was fixed to the human value, i.e. about 67% of GFR (44). Bladder compartment was used as a transitory compartment receiving urine from tubular lumen and evacuating it, with an exit flow (Quri) determined in pigs kept in metabolism cage. This compartment was not considered as a vascularized tissue (no distribution).

For IM administrations, a compartment of depot was added (45). Two absorption rate constants originating from this depot compartment to the venous one were estimated, one for CMS (K_{IM_CMS}) and one for colistin (K_{IM_COLI}). Intrinsic hydrolysis of CMS and elimination of colistin were supposed to occur in this compartment such as in all other compartments (Fig. 1C).

The control file describing the PBPK model is presented in the supplementary files.

- Model calibration and modelling method

A NLME modelling approach was used for the estimation of unknown parameters, inter-individual variabilities (IIV) and residual variabilities (RV) (19). Model structure was modified if needed and model selection was based on the physiological plausibility (as described above) and a parsimonious approach. A decrease of the objective function value (OFV) of more than 3.84, corresponding to a 5% significance level, was considered as a significant improvement in model fit. The sampling importance resampling (SIR) method (46) was used to obtain the 95% confidence intervals (IC 95%) of the parameter estimates (5 iterations with 1000, 1000, 1000, 2000, 2000 samples and 200, 400, 500, 1000, 1000 resamples for each).

For IIV, a log-normal distribution of parameters was assumed. IIV was firstly estimated for each parameter separately and retained only if a significant decrease in OFV was observed without adding uncertainties in the estimation of fixed effects (forward selection process). In a second step, all IIV parameters for which the p-value was <0.05 in the univariate analysis were included in the model, and a stepwise backward selection was then performed, with a threshold of p-value of <0.05. .

For RV, additive and proportional error structure models were tested. Furthermore, for CMS and colistin concentrations determined in the same sample (see details of the analytical method), the L2 data item method was used in order to estimate potential correlation between their RV (47). The M3 method was used to handle data below the LOQ (BLOQ) (48).

The calibration step was performed with all experimental data described in section "Experimental setup for model calibration" and summarized in Table I. Concentrations were log-transformed before modelling. For urine data, CMS and colistin could not be discriminated due to the spontaneous hydrolysis of CMS into colistin after excretion (2, 6). Thus, all observed concentrations were converted as CMS quantities (thanks to molecular ratio and measured urine volume) and pooled. Accordingly, urinary CMS and colistin model predictions were also pooled. Predictions in kidney corresponded to the amount of colistin and CMS in the different kidney sub-compartments (vascular, extra-vascular, intracellular and tubular lumen) divided by the sum of their respective volumes. Moreover, colistin and CMS concentrations in kidney were pooled for the analysis (*cf*. analytical methods).

The determination of CMS and colistin half-lives in plasma and kidneys was done by graphical identification of the different phases of decrease for predicted concentrations in log-scale, and then by calculating the time required for the typical concentrations to decrease by 50% in each phase. Total clearances of each compound were calculated as the dose of CMS, or as the total formed quantity of colistin, divided by the area under the curve of the plasma CMS, or colistin concentration, respectively. The renal clearances (CL_R) in this study accounted for the removal of compounds in kidney by different routes, *i.e.* secretion/excretion processes and hydrolysis of CMS or degradation of colistin. Thus, they were defined as the product of renal extraction ratio by the renal flow (Q_{kid}):

$$CL_R = \frac{(C_{art} - C_{kid\_VA})}{C_{art}} . Q_{kid} \quad \text{(Eq. 4)}$$

With C_{art}: arterial concentration of CMS or colistin; C_{kid_VA}: concentrations of CMS or colistin in renal vascular compartment.

- <u>Model evaluation</u>

The performances of the PBPK model were tested in a 2-step approach. An internal validation was firstly done based on graphical and statistical criteria. Goodness-of-fit was assessed by plotting

observed (DV) versus individual predictions (IPRED) and population predictions (PRED). Then Visual Predictive Checks (VPC) were generated, stratified by experimental designs and organs, with 1000 simulated replicates from the calibration dataset (Experiments n°1 to n°4, see Table I). The 5^{th} and 95^{th} percentile of the model predictions were plotted to check if 90% of the experimental data were included within this interval.

Then, an external validation was done with the independent dataset that was not used for calibration (Experiment n°5). This experiment followed the recommended veterinarian CMS doses. All parameters estimated during model calibration (fixed and random effects) were fixed. No RV was estimated for concentrations in tissues (except kidneys) during calibration because these tissue data were only used to determine the CMS and colistin Kps. Therefore, a common RV value between those estimated in plasma and kidney was chosen for the predictions of colistin concentrations in all other tissues. Concentrations of CMS and colistin within each organ were simulated with the final model and the predictive ability of the PBPK model was assessed by visualizing the distribution of the validation dataset within the 90% prediction intervals (10% of the data expected to be outside the interval). Only compartments involved in withdrawal period calculations (fat, skin, muscles, liver and kidney) and plasma were analysed.

A local sensitivity analysis was performed on the estimated structural parameters to assess their influence (associated to potential uncertainties) on model predictions. This analysis was performed only for kidney predictions, which was the main tissue of interest. The sensitivity analysis consisted in a ± 10% perturbation of each parameter estimate, all other parameters estimate being unchanged. The output considered for sensitivity was the time when the median model prediction for concentration in kidney felt below its MRL (0.20 µg/g).

- <u>Model application: Withdrawal period estimation</u>

To estimate withdrawal period, we generated a 98 % prediction interval (*i.e.* 99% unilateral) (49) from 1000 simulations of the individual predicted profiles (without RV) of virtual pigs of 50 kg receiving the dosing scheme of CMS used in veterinary medicine. Then, the same approach was done with a virtual pig of 100 kg (which is close to the real slaughter weight). These simulations were performed with all structural parameters and their IIV (if present) estimated with the final model. Times for which the upper prediction limit felt below the MRL for each tissue intended for human consumption were determined. Then, the highest time from all of them was chosen as the final withdrawal period.

Software

The modelling was performed using NONMEM 7.4 (ICON Development Solutions, Ellicott City, Maryland, USA) with the first order conditional estimation method including eta-epsilon interaction (FOCE-I) and ADVAN 14. Perl speaks NONMEM (50) and Piraña (51) were used in order to facilitate the modelling work. All graphs were done using R software (version 3.4.1, www.R-project.org).

RESULTS

- Unbound fraction of CMS in plasma

We experimentally determined the $fu_{\_CMS}$ by ultra-filtration at 37°C (Table III). About 28 % of CMS was lost in buffer solution due to the CMS hydrolysis and to the non-specific binding to the tube. The measurement of colistin concentrations in the buffer samples at 37 °C indicated that less than 6% of CMS was hydrolysed into colistin after 30 min (data not shown). Moreover, we had previously estimated in human and rat plasma samples spiked with CMS and kept for 30 min at 37°C, that about 8% of CMS was converted into colistin (in-house data). Therefore, the hydrolysis of CMS in plasma and buffer were quite low over the period of this experiment (30 min) and could be considered as negligible. Overall, by neglecting the degradation of CMS into colistin and assuming that the non-

425 specific binding was similar during the ultrafiltration experiments in plasma and buffer, the average
426 $fu_{\_CMS}$ was estimated to be 37 ± 3 % in pigs.

427

428 • Model structure and calibration

429 The structure of the base model was developed in order to fit the experimental data. Colistin Kps were
430 calculated as the ratios of concentrations measured at steady-state in tissue and plasma. However, for
431 muscles, 3 concentrations over 6 were below the LOQ and were fixed at LOQ/2 for calculations of Kps.
432 Results for Kps of colistin are reported in Table II. Concerning Kps of CMS, about 80% of tissue
433 concentrations (except kidney) were under the LOQ (1 µg/g of tissue) at steady-state. Therefore, these
434 Kps could not be measured experimentally and were estimated by the model (M3 method for data
435 below the LOQ). However, estimation of one specific Kp for each organ was impossible and a Kp of
436 CMS common for all tissues (Kp_{mix_CMS}) as well as a common RV value for CMS concentrations in
437 tissues were estimated (except for kidneys).

438 One additional compartment was added to each vascular compartment (arteries and veins) in
439 order to fully describe the plasma colistin kinetic profile. These two compartments, referred as "deep
440 compartments", were volume-less and with two different estimated transfer constants (K_{DEEP_COLI}
441 and $K_{DEEP\_OUT\_COLI}$) (Fig. 1D).

442 Structural modifications were needed for the kidney sub-model (permeability-limited model). Due
443 to the protein binding of CMS, a secretion clearance of CMS (CL_{sec_CMS}) from the extra-vascular
444 compartment towards the tubular lumen through the intracellular compartment was added to explain
445 the urinary excretion of CMS (Fig. 2). A rate of degradation of colistin ($K_{deg\_COLI)}$ in kidneys different
446 from that in other organs was estimated but did not improve significantly the fitting. Non-linear
447 mechanisms for renal elimination of colistin were also tested, without significant improvement of the
448 fitting. An intracellular binding compartment (volume less) significantly improved the fitting (OFV
449 decrease of 20), with two different estimated "in and out" transfer constants (K_{ON_COLI} and

450 K_{OFF_COLI}). Because CMS and colistin could not be distinguished in urine, the fraction of colistin
451 reabsorbed in proximal tubules could not be accurately estimated. Therefore, the proportion of colistin
452 reabsorbed (driven by CL_{reabs_COLI}) was estimated from data in human healthy volunteers (6) and
453 fixed at 97.5%.
454
455 The parameter estimates of the PBPK model after model calibration are reported in Table IV. For each
456 structural parameter, CI 95 % were satisfying (the wider interval being for the colistin absorption
457 constant from IM depot, K_{IM_COLI}) highlighting the good precisions of the estimates. Overall,
458 uncertainty for CMS parameters was lower than for colistin ones. Proportional residual errors were
459 chosen as the best error models and the highest estimated RV was for kidney concentrations (57%).
460 Two inter-individual variabilities, one associated to K_{deg_COLI} (26.6%) and the other to CL_{SEC_CMS}
461 (43.5%), were estimated.
462
463 • Model evaluation

464 Model diagnostics showed acceptable goodness-of-fit plot for the final model (supplementary
465 material, Fig. S1). The VPCs generated for the internal validation showed a good agreement between
466 model median predictions and CMS and colistin concentrations measured in plasma, either after one
467 IV of CMS (experiment n°1, Fig. 3A), one IM of CMS (experiment n°2, Fig. 3B) or after the dosing
468 regimen implemented to achieve steady-state (experiment n°3, Fig. 4A). Median predictions of plasma
469 concentrations were also reasonably well described after repeated IM administrations (experiment
470 n°4, Fig 4B), even if the median predictions were slightly below the measured peak of plasma
471 concentrations for both compounds. However, distribution and elimination phases were well fitted.
472 The wide prediction intervals, though, highlighted that variability could be overestimated. Overall,
473 data BLOQ were well predicted by the model as shown on Fig 3A and 3B. For the repeated IM
474 injections, collected data were sparse so the fractions of data BLOQ were not presented due to

475 graphical reasons. However, the only discrepancy was at 9 h just before the second IM injection
476 because all observed colistin data were BLOQ in contrast to the model prediction (Fig 4B).

477 Concerning kidney sub-model, cumulative urinary amounts after one IV administration of CMS were
478 well predicted by the model (Fig. 5). For concentrations in kidney, the typical prediction captured well
479 the renal accumulation (Fig. 6C), but there was a high variability between the different experiments,
480 with some under-predictions (Fig. 6B) or over-predictions (Fig. 6A and late points of Fig. 6C). This
481 variability was taken into account by the model thanks to the high estimated IIV and RV. However, the
482 large 90% PI suggest that variability could be overestimated in kidneys.
483
484 To assess the PBPK model predictive ability, an external validation was performed with an independent
485 dataset that was not used during model calibration. Median plasma concentrations of both
486 compounds were quite well fitted by the model typical predictions (Fig. 7). In kidneys, the elimination
487 phase was in good match with observed data (Fig. 8) but the typical prediction under-estimated the
488 maximal concentrations. For other tissue concentrations, most of the observed data were below the
489 LOQ for CMS and colistin (Supplementary files, Fig. S2 and S3) and this was well predicted by the model.
490 However, typical concentrations of CMS in muscles and of colistin in skin were slightly under-predicted.
491 Overall, these results gave good confidence in the PBPK model predictive ability, even if there was a
492 slight overestimation of the total variability.
493
494 • <u>CMS and colistin pharmacokinetics in plasma and tissue</u>

495 After IV and IM injections of CMS, plasma concentrations of CMS declined quickly and were under the
496 LOQ 8 h post-administration (Fig 3A and 3B). By contrast, colistin plasma concentrations declined
497 slower and were still quantifiable more than 24 h after CMS administration. The estimated half-life
498 ($t_{1/2}$) of CMS was 1.2 h. For colistin, an initial (lasting from 0 to 10 h after dosing) half-life of distribution
499 of 1.8 h was calculated, followed by a terminal half-live of 10.5 h. This terminal $t_{1/2}$ for colistin was

described in the model thanks to the additional deep compartments. The maximal concentrations of colistin were predicted to occur 1 h after the end of the IV infusion, or 2 h after IM injection. As shown by the median prediction in figure 4A, the plasma steady-state of CMS and colistin was achieved at the end of experiment n°3 for Kp determination, thanks to the use of a loading dose of CMS. Concerning drug elimination, total CMS clearance was estimated to 11.6 L/h for a virtual pig of 50 kg, whose 7.9 L/h was associated to renal clearance, which included the glomerular filtration, the tubular secretion and the CMS hydrolysis within kidneys. For colistin, the total clearance was found to be at 7.4 L/h whereas the renal clearance, which was mostly due to intracellular metabolism, accounted for 1.5 L/h (see below).

For tissues other than kidneys, all colistin Kp values were less than one (Table II) as well as the common estimated Kp for CMS (Table IV). In kidneys, the CMS concentrations were predicted to decrease quickly after an administration of CMS (Supplementary material, Fig. S4). Therefore, we can consider that at late time points after administration there was only colistin remaining in kidneys. Residual renal concentrations were still high 31 h after the single IV injection (7.0 ± 3.4 µg/g, Fig. 6A) and 63 h after the last IM injection (5.6 ± 1.9 µg/g, Fig. 6C); the terminal $t_{1/2}$ of colistin in kidneys was estimated to be about 38 h. After twice daily IM administrations of CMS 25,000 UI/kg, colistin concentrations in kidney were 7.0 ± 1.3 µg/g after 1 day (2 doses), 14.7 ± 9.9 µg/g after 3 days (6 doses) and 24.6 ± 5.9 µg/g after 7 days (14 doses) (experiment n°4, Fig. 6C). The model predicts that steady-state in kidney should be almost reached after 5 days of treatment.

The relative disposition of CMS and colistin within the kidneys as predicted by the PBPK model is presented on Figure 9. Typically, 68% of the initial dose is predicted to be excreted in urine as a mix of CMS and colistin, with 56% due to the net tubular secretion of CMS and only 12% due to the glomerular filtration of CMS. In urine, CMS accounted for more than 99% of the total quantities. Among the fraction of the CMS dose converted into colistin (32%), only 2% were converted into the kidney. Colistin extraction ratio in kidney would be 18%, with glomerular filtration of the unbound fraction in plasma,

almost complete reabsorption (0.2% of formed colistin excreted in urine) and intracellular degradation in proximal tubules. Overall, kidneys would account for 20% of total colistin clearance.

For the other compartments, the evolution of the mass balance of CMS and colistin after one IV of CMS are represented in the supplementary materials (Fig. S5).

- Model application: withdrawal period estimation

The withdrawal period was calculated from depletion in kidneys because colistin concentrations within this organ remained the longest above the LMR. The simulation of the PBPK model gave a WP of 23 days for a virtual pig of 50 kg (Fig. 10) and 25 days for a virtual pig of 100 kg (Supplementary material, Fig. S6). The sensitivity analysis revealed that K_{ON_COLI} , K_{OFF_COLI} and K_{deg_COLI} were the 3 parameters that particularly influenced the output, *i.e.* the time when the median model prediction of the renal concentration fell below the MRL. The most influential parameter was K_{OFF_COLI}, because 10 % variation of its value caused 8 % to 9 % variation of the output (Table V).

DISCUSSION

A whole body PBPK model was developed for colistin and its pro-drug, CMS, with a nonlinear mixed effect modelling approach. This model could reasonably well predict the median CMS and colistin concentrations in plasma (Fig. 7) and tissues, especially for kidneys (Fig. 8). For pigs, the PK of CMS in plasma was monophasic, with a $t_{1/2}$ of 1.2 h, whereas the PK of colistin was biphasic, with a distribution $t_{1/2}$ of 1.8 h and a terminal $t_{1/2}$ of 10.5 h (Fig 3A and 3B). These half-lives in pigs were in good agreement with those in healthy volunteers (6) except that a monophasic elimination of colistin was described. However, this biphasic profile was also observed in sheep, another large-animal model (52). As colistin is known to non-specifically bind to biological and non-biological matrix (7, 53, 54), deep compartments linked to vascular ones were implemented in the PBPK model to fit the plasma

concentrations of colistin at late time points. These compartments may reflect either a permeability-limited distribution of colistin in some organs, *e.g.* due to a weak intracellular penetration, or a high affinity binding to some extracellular component (*e.g.* red blood cells (55)), thus resulting in a slow release of colistin towards plasma. However, evidences of these mechanisms should be sought in experimental studies.

Concerning distribution, plasma unbound fraction of CMS was determined for the first time in pigs, thanks to an ultra-filtration method and by taking care of CMS degradation and potential adsorption to laboratory material. This value (37%) was close to that of colistin (40%) found in literature for pigs (25), highlighting a non-negligible protein binding. Colistin is known to bind to α-1-acid glycoprotein (at least for human) due to its cationic properties (56) but the mechanisms of CMS protein binding have not been investigated yet. Regarding tissue distribution, all Kp values (experimental ones for colistin and estimated ones for CMS) were lower than 1. This result reflected a poor distribution into tissues that could be in accordance with an extracellular distribution of CMS and colistin within organs. Our values were in good agreement with the experimental Kps determined in rats for colistin (18), suggesting that these values could be used for inter-species extrapolations.

Concerning the elimination, CMS total clearance was higher (0.23 L/h/kg) than the colistin one (0.15 L/h/kg) for a standard pig weighting 50 kg. These results compare favourably with previous results in pigs (57). By contrast, these clearances are greater than those reported in healthy volunteers for CMS and colistin (0.12 L/h/kg and 0.040 L/h/kg for a man weighting 73 kg, respectively) (6), which is in contradiction with the classical allometry scaling laws based on weight (58). Therefore, extrapolation of clearances between the two species may be challenging.

To our knowledge, this is the first time that an accumulation of colistin in kidneys was quantified over time after repeated CMS administrations. Indeed, after a twice-daily IM administration of CMS (50,000 UI/kg/day) for 7 days, colistin concentrations in kidney were more than 3-fold higher than after the first administration (Fig. 6C). This was related to the long $t_{1/2}$ of colistin estimated in this

577 organ (~38 h). A previous study in rats already attested that the concentrations of colistin were high in
578 kidney after 7 days of treatment (65.7 fold higher than in plasma), but the renal accumulation was not
579 investigated over time (59).

580 To go further into the underlying mechanisms of the renal disposition of CMS and colistin, we
581 divided the kidney into physiological sub-compartments (Fig. 2) (43). The unbound fraction of CMS in
582 plasma, estimated herein, implied a tubular secretion of CMS because glomerular filtration was
583 insufficient to explain the amounts measured in urine (Fig. 2). According to our model, this tubular
584 secretion was the major elimination pathway for CMS in kidney, 4 to 5-fold higher than glomerular
585 filtration (Fig. 9). This net tubular secretion of CMS into urine was already supported by studies in rats
586 (2) and suggested in humans (60), but as the unbound fraction of CMS in plasma was unknown, it
587 remained hypothetic. The median proportion of the initial dose of CMS excreted in urine was predicted
588 to be 68 %, in accordance with the 60 to 70 % of CMS dose recovered in urine in rats and humans (2,
589 6).

590 Regarding colistin pharmacokinetics in kidneys, the tubular reabsorption is known to be
591 career-mediated thanks to PEPT2 and megalin (10, 14). In our model, the clearance of reabsorption
592 from the tubular lumen (CL_{reabs_COLI}) was fixed to a physiological value estimated from data in man
593 (6), due to an identifiability problem. This reabsorption explained the colistin accumulation within
594 tubular cells and the very small amount of colistin excreted in urine. Colistin might also undergo a
595 tubular secretion, as for CMS, but because of the predominant reabsorption, this was not identifiable
596 by our model.

597 Several hypotheses were considered in the model to describe the colistin accumulation in
598 kidneys and its slow elimination in this organ. For instance, we tried to estimate a different colistin
599 intrinsic constant of elimination (K_{deg_COLI}) in kidney, or to estimate a release of colistin from the
600 kidneys towards the systemic circulation. However, these hypotheses did not improve the fitting or
601 parameters were not identifiable. Moreover, the latter assumption, besides the modelling results, was
602 also in contradiction with the results of previous studies showing *in vivo* that when the reabsorption

603 of colistin or polymyxin B in renal tubules was inhibited, the renal exposures was reduced considerably
604 but the kinetic profiles in plasma remained unaltered (10, 61). The fact that total clearance of
605 polymyxin remained unchanged, whether the reabsorption was inhibited or not, suggested that
606 polymyxin was eliminated within the kidney, either excreted in urine or metabolized, but did not go
607 back to the systemic circulation. Finally, the use of a renal intracellular "binding" compartment, with a
608 slow release, was the best choice for the goodness-of-fit and for physiological reasons. Indeed, the
609 observed colocalization with cell organelles (12) and the known non-specific binding properties of
610 polymyxins to cellular membranes (1) could support this assumption. Sensitivity analysis suggested
611 that these intracellular binding parameters were the parameters that most influenced the kidney
612 exposure to colistin (Table V). This kind of intracellular binding has already been presented in another
613 PBPK model developed and validated for doxorubicin (belonging to an antitumor antibiotic family) (30).
614 Furthermore, due to this intracellular accumulation, about 20 % of the total formed colistin quantities
615 were predicted to be metabolized within the kidneys, highlighting a major role of kidneys in colistin
616 elimination. Further *in vitro* studies should be performed to investigate this intracellular binding and
617 the intra-renal elimination.
618
619 These new renal data, about CMS tubular secretion and colistin accumulation over time, may
620 be useful to explore the nephrotoxicity associated to the use of CMS and colistin. Indeed, in a recent
621 meta-analysis, nephrotoxicity ranged from 24% to 74% in CMS-treated patients but most of the events
622 were reversible (62). The duration therapy and the daily dose are risk factors of renal toxicity (1). In
623 our study, the renal steady-state was quasi-achieved after 5 days of treatment (>120 h) and high renal
624 concentrations were reached (>20 µg/g) (Fig. 6C). However, no clinical sign of renal insufficiency was
625 observed in our animals and the creatinine concentrations in plasma stayed within the normal range
626 over the whole treatment period (data not shown). Nevertheless, measurement of other biomarkers
627 (like urinary creatinine or plasma cystatin C) might have been better to detect early signs of
628 nephrotoxicity (63), in addition to histological analysis. According to modelling results, the intra-renal

conversion of CMS into colistin was very minor compared to the colistin that was reabsorbed and accumulated inside tubular cells. The accumulation of polymyxin inside proximal tubular cells is supposed to be responsible for the nephrotoxic effects involving apoptosis and oxidative stress (15, 16). However, the model slightly underestimated peak concentrations in kidney (Fig. 8), which may be of importance for nephrotoxic predictions. Of note, a high amount of CMS (56% of initial dose) transited inside tubular cell. This is important as CMS (and its numerous partially methanesulfonated derivatives) is invoked as a potential contributor to the observed nephrotoxic effects (60). Nevertheless, this model could be refined when new data will be available.

As a model application, we chose to estimate the withdrawal period (WP) after IM injections of CMS in pigs following the veterinarian recommended doses. WP is defined as the time after last administration for which 99 % of animals have residual edible tissue concentrations below the MRL, in Europe. Kidney was the tissue of interest because of the accumulation and of the slow colistin depletion (Fig. 8), compared to all other edible tissues (Supplementary files, Fig. S2 and S3). Simulations from the PBPK model gave an estimated WP of 23 days for a 50-kg pig. Since our last experimental concentration was measured 3 days after last administration, further experimental data around the estimated WP would have been preferable to confirm it. Overall, the model prediction seemed reasonable as our estimated WP (23 days) was close to the official one given in the summary of product characteristics of the veterinary medicinal product (21 days). The renal accumulation observed in our repeated CMS injections experiment highlighted that an extra label use of CMS would probably need longer WP. No data of such use for colistin are currently recorded but the use of PBPK models in these extra label situations has already proved its interest (64). Furthermore, this PBPK model was developed with colistin and its prodrug CMS but it could be easily adapted to pigs injected directly with colistin, as possibly done in veterinary medicine (65).

To our knowledge, this is the first study using a NLME approach for a PBPK model related to withdrawal period calculation. The process of PBPK models development for food safety is well

655 established as explained in a recent review of veterinary pharmacology (23). This method allows to
656 predicting the time course of drug concentrations in any tissue of interest. Different doses and route
657 of administrations can be used to develop a PBPK model as we did, enhancing its robustness of
658 prediction (23). The classical statistical methodology for WP estimation uses inferences on a limited
659 number of healthy animals whereas the real-life target is diseased animals. We also used healthy
660 animals but the PBPK model can easily handle patho-physiological changes of parameters, like for a
661 diseased animal, to see the effect on tissue drug concentrations. In addition, the use of NLME
662 modelling brings many advantages. Noticeably, it gives estimation of population variabilities like inter-
663 individual variability, which is discriminated from the unexplained but quantified residual variability.
664 This is important as the WP calculation applies for a global "population of treated animals" and must
665 include 99% of them. The prediction of WP was based on simulations taking into account IIV but not
666 RV, because what is important is the actual concentration in tissue (which depends on IIV) and not the
667 measured concentration (which depends also on RV). As there was only one tissue sample per animal
668 (destructive sampling), IIV might be difficult to estimate and it is possible that RV, which was high for
669 renal concentrations (57%), was inflated by unidentified IIV. This bias, resulting in an underestimation
670 of the IIV, could result in an underestimation of the WP. On the other hand, VPCs indicated that there
671 was a potential overestimation of the overall variability, without knowing if it was IIV or RV that was
672 inflated: this bias would result in a contrary over-prediction of WP. This issue rises the necessity, for
673 an accurate estimation of WP, of an accurate estimation of both IIV and RV. The NMLE approach is also
674 efficient to handle sparse data (like in experiment n°4) and thus could limit the number of necessary
675 animals. Furthermore, this method allows a sophisticated handling of data below the limit of
676 quantification compared to the classic one. Indeed, in the latter approach, the rule is to omit or fix the
677 data BLOQ at half of the LOQ but it could bias the results (22).
678
679 Lastly, it is necessary to highlight some analytical considerations. Due to the high instability of
680 CMS, direct measure of its concentration was not possible (26). The indirect method used could not

discriminate renal CMS and colistin concentrations, which were pooled. Therefore, the estimations of parameters in kidney might have been biased. Moreover, CMS is a mixture of many methanesulfonated derivatives carrying various number of methanesulfonate groups (3). It was not possible to determine the concentration of each component separately; therefore, all these derivatives were considered as being CMS. As previously explained, colistin (which has no methanesulfonate group) is widely reabsorbed, whereas CMS (which have 5 methanesulfonate groups) is not. Therefore, some partially methanesulfonated derivatives, *i.e.* considered as CMS, might also be reabsorbed. These compounds may have an ADME closer to colistin than to CMS. All these concerns highlight the need of further analytical developments allowing to discriminate CMS and colistin in kidneys and to quantify the various methanesulfonate derivatives.

CONCLUSION

To conclude, this PBPK model coupled with a NMLE approach gave new insight into the mechanistic pharmacokinetics of CMS and colistin, especially within kidneys. This may have implications to limit the colistin induced-nephrotoxicity in human medicine. We also used this model to estimate withdrawal period in pigs treated with CMS, highlighting the utility of such an approach in veterinary medicine. Furthermore, PBPK models are helpful to perform inter-species extrapolation (from animal to human), but also intra-specie extrapolation (from adult to children). Thus, this model could be useful to adapt CMS dosing-regimen in pediatric population, a sub-population which is less studied. Some works about this topic are ongoing in our team.

Acknowledgments

Alexis Viel was supported by a doctoral fellowship from the French National Institute of Health and Medical Research (Inserm) and the French Agency for Food, Environmental and Occupational Health & Safety (Anses).

REFERENCES

1. Gregoire N, Aranzana-Climent V, Magreault S, Marchand S, Couet W. Clinical Pharmacokinetics and Pharmacodynamics of Colistin. Clinical pharmacokinetics. 2017.
2. Li J, Milne RW, Nation RL, Turnidge JD, Smeaton TC, Coulthard K. Pharmacokinetics of colistin methanesulphonate and colistin in rats following an intravenous dose of colistin methanesulphonate. The Journal of antimicrobial chemotherapy. 2004;53(5):837-40.
3. Li J, Milne RW, Nation RL, Turnidge JD, Coulthard K. Stability of Colistin and Colistin Methanesulfonate in Aqueous Media and Plasma as Determined by High-Performance Liquid Chromatography. Antimicrobial Agents and Chemotherapy. 2003;47(4):1364-70.
4. Forrest A, Garonzik SM, Thamlikitkul V, Giamarellos-Bourboulis EJ, Paterson DL, Li J, et al. Pharmacokinetic/toxicodynamic analysis of colistin-associated acute kidney injury in critically ill patients. Antimicrobial Agents and Chemotherapy. 2017:AAC. 01367-17.
5. Li J, Nation RL, Milne RW, Turnidge JD, Coulthard K. Evaluation of colistin as an agent against multi-resistant Gram-negative bacteria. Int J Antimicrob Agents. 2005;25(1):11-25.
6. Couet W, Gregoire N, Gobin P, Saulnier P, Frasca D, Marchand S, et al. Pharmacokinetics of colistin and colistimethate sodium after a single 80-mg intravenous dose of CMS in young healthy volunteers. Clinical Pharmacology & Therapeutics. 2011;89(6):875-9.
7. Craig WA, Kunin CM. Dynamics of binding and release of the polymyxin antibiotics by tissues. J Pharmacol Exp Ther. 1973;184(3):757-65.
8. Tomasi L, Giovannetti L, Rondolotti A, Rocca GD, Stracciari GL. Depletion of the residues of colistin and amoxicillin in Turkeys following simultaneous subcutaneous administration. Veterinary research communications. 1996;20(2):175-82.
9. Ma Z, Wang J, Nation RL, Li J, Turnidge JD, Coulthard K, et al. Renal disposition of colistin in the isolated perfused rat kidney. Antimicrobial agents and chemotherapy. 2009;53(7):2857-64.
10. Suzuki T, Yamaguchi H, Ogura J, Kobayashi M, Yamada T, Iseki K. Megalin contributes to kidney accumulation and nephrotoxicity of colistin. Antimicrobial agents and chemotherapy. 2013;57(12):6319-24.
11. Yun B, Azad MA, Wang J, Nation RL, Thompson PE, Roberts KD, et al. Imaging the distribution of polymyxins in the kidney. Journal of Antimicrobial Chemotherapy. 2014:dku441.
12. Yun B, Azad MA, Nowell CJ, Nation RL, Thompson PE, Roberts KD, et al. Cellular uptake and localization of polymyxins in renal tubular cells using rationally designed fluorescent probes. Antimicrobial agents and chemotherapy. 2015;59(12):7489-96.
13. Azad MA, Roberts KD, Yu HH, Liu B, Schofield AV, James SA, et al. Significant accumulation of polymyxin in single renal tubular cells: a medicinal chemistry and triple correlative microscopy approach. Analytical chemistry. 2015;87(3):1590-5.
14. Lu X, Chan T, Xu C, Zhu L, Zhou QT, Roberts KD, et al. Human oligopeptide transporter 2 (PEPT2) mediates cellular uptake of polymyxins. Journal of Antimicrobial Chemotherapy. 2015.

15. Dai C, Li J, Tang S, Li J, Xiao X. Colistin-induced nephrotoxicity in mice involves the mitochondrial, death receptor, and endoplasmic reticulum pathways. Antimicrob Agents Chemother. 2014;58(7):4075-85.
16. Azad MA, Akter J, Rogers K, Nation RL, Velkov T, Li J. Major pathways of polymyxin-induced apoptosis in rat kidney proximal tubular cells. Antimicrob Agents Chemother. 2015.
17. Nestorov I. Whole-body physiologically based pharmacokinetic models. Expert opinion on drug metabolism & toxicology. 2007;3(2):235-49.
18. Bouchene S, Marchand S, Couet W, Friberg LE, Gobin P, Lamarche I, et al. Comparison of Colistin and Colistimethate sodium (CMS) Model-Predicted Whole-Body Distribution with Measured Tissue:Plasma Concentrations Ratios in Rats. 53 rd Interscience Conference on Antimicrobial Agents and Chemotherapy; Denver, CO2013.
19. Sheiner LB, Beal SL. Evaluation of methods for estimating population pharmacokinetic parameters II. Biexponential model and experimental pharmacokinetic data. Journal of Pharmacokinetics and Pharmacodynamics. 1981;9(5):635-51.
20. Swindle MM, Makin A, Herron AJ, Clubb FJ, Frazier KS. Swine as Models in Biomedical Research and Toxicology Testing. Veterinary Pathology Online. 2012;49(2):344-56.
21. JECFA. Residue Evaluation of Certain Veterinary Drugs: Joint FAO/WHO Expert Committee on Food Additives, 66th Meeting 2006: Food & Agriculture Org.; 2006.
22. EMA. Guideline on approach towards harmonisation of withdrawal periods. European Medicines Agency (EMA) - Committee for Medicinal Products for Veterinary Use (CVMP), 2016 EMA/CVMP/CHMP/231573/2016 Contract No.: EMA/CVMP/SWP/735325/2012.
23. Lin Z, Gehring R, Mochel J, Lavé T, Riviere J. Mathematical modeling and simulation in animal health–Part II: principles, methods, applications, and value of physiologically based pharmacokinetic modeling in veterinary medicine and food safety assessment. Journal of veterinary pharmacology and therapeutics. 2016;39(5):421-38.
24. Nation RL, Li J, Cars O, Couet W, Dudley MN, Kaye KS, et al. Consistent Global Approach on Reporting of Colistin Doses to Promote Safe and Effective Use. Clinical Infectious Diseases. 2014;58(1):139-41.
25. Rottbøll LAH, Friis C. Penetration of antimicrobials to pulmonary epithelial lining fluid and muscle and impact of drug physicochemical properties determined by microdialysis. Journal of pharmacological and toxicological methods. 2016;78:58-65.
26. Gobin P, Lemaître F, Marchand S, Couet W, Olivier J-C. Assay of Colistin and Colistin Methanesulfonate in Plasma and Urine by Liquid Chromatography-Tandem Mass Spectrometry. Antimicrobial Agents and Chemotherapy. 2010;54(5):1941-8.
27. Buur JL, Baynes RE, Craigmill AL, Riviere JE. Development of a physiologic-based pharmacokinetic model for estimating sulfamethazine concentrations in swine and application to prediction of violative residues in edible tissues. American journal of veterinary research. 2005;66(10):1686-93.
28. Chen K, Seng KY. Calibration and validation of a physiologically based model for soman intoxication in the rat, marmoset, guinea pig and pig. Journal of applied toxicology : JAT. 2012;32(9):673-86.
29. de Boer VC, Dihal AA, van der Woude H, Arts IC, Wolffram S, Alink GM, et al. Tissue distribution of quercetin in rats and pigs. The Journal of nutrition. 2005;135(7):1718-25.
30. Dubbelboer IR, Lilienberg E, Sjögren E, Lennernas H. A model-based approach to assessing the importance of intracellular binding sites in doxorubicin disposition. Molecular Pharmaceutics. 2017;14(3):686-98.
31. Elowsson P, Carlsten J. Body composition of the 12-week-old pig studied by dissection. Laboratory animal science. 1997;47(2):200-2.
32. Eskild-Jensen A, Jacobsen L, Christensen H, Frokiaer J, Jorgensen HS, Djurhuus JC, et al. Renal function outcome in unilateral hydronephrosis in newborn pigs. II. Function and volume of contralateral kidneys. J Urol. 2001;165(1):205-9.

33. Lødrup AB, Karstoft K, Dissing TH, Nyengaard JR, Pedersen M. The association between renal function and structural parameters: a pig study. BMC Nephrology. 2008;9:18-.
34. Lundeen G, Manohar M, Parks C. Systemic distribution of blood flow in swine while awake and during 1.0 and 1.5 MAC isoflurane anesthesia with or without 50% nitrous oxide. Anesthesia and analgesia. 1983;62(5):499-512.
35. Rendas A, Branthwaite M, Reid L. Growth of pulmonary circulation in normal pig--structural analysis and cardiopulmonary function. Journal of Applied Physiology. 1978;45(5):806-17.
36. Scotcher D, Jones C, Posada M, Rostami-Hodjegan A, Galetin A. Key to Opening Kidney for In Vitro–In Vivo Extrapolation Entrance in Health and Disease: Part I: In Vitro Systems and Physiological Data. The AAPS journal. 2016;18(5):1067-81.
37. Suenderhauf C, Parrott N. A physiologically based pharmacokinetic model of the minipig: data compilation and model implementation. Pharmaceutical research. 2013;30(1):1-15.
38. Ten have GAM, Bost MCF, Suyk-Wierts JCAW, van den Bogaard AEJM, Deutz NEP. Simultaneous measurement of metabolic flux in portally-drained viscera, liver, spleen, kidney and hindquarter in the conscious pig. Laboratory Animals. 1996;30(4):347-58.
39. Tranquilli WJ, Manohar M, Parks CM, Thurmon JC, Theodorakis MC, Benson GJ. Systemic and regional blood flow distribution in unanesthetized swine and swine anesthetized with halothane + nitrous oxide, halothane, or enflurane. Anesthesiology. 1982;56(5):369-79.
40. Upton RN. Organ weights and blood flows of sheep and pig for physiological pharmacokinetic modelling. Journal of Pharmacological and Toxicological Methods. 2008;58(3):198-205.
41. Vinegar A. Development of a physiologically based pharmacokinetic model for the anesthetics halothane, isoflurane, and desflurane in the pig (Sus scrofa). DTIC Document, 1999.
42. Drougas JG, Barnard SE, Wright JK, Sika M, Lopez RR, Stokes KA, et al. A model for the extended studies of hepatic hemodynamics and metabolism in swine. Laboratory animal science. 1996;46(6):648-55.
43. Peters SA. Physiologically-based pharmacokinetic (PBPK) modeling and simulations: principles, methods, and applications in the pharmaceutical industry: John Wiley & Sons; 2012.
44. Scotcher D, Jones C, Rostami-Hodjegan A, Galetin A. Novel minimal physiologically-based model for the prediction of passive tubular reabsorption and renal excretion clearance. European Journal of Pharmaceutical Sciences. 2016;94:59-71.
45. Leavens T, Tell L, Clothier K, Griffith R, Baynes RE, Riviere J. Development of a physiologically based pharmacokinetic model to predict tulathromycin distribution in goats. Journal of veterinary pharmacology and therapeutics. 2012;35(2):121-31.
46. Dosne A-G, Bergstrand M, Harling K, Karlsson MO. Improving the estimation of parameter uncertainty distributions in nonlinear mixed effects models using sampling importance resampling. Journal of pharmacokinetics and pharmacodynamics. 2016;43(6):583-96.
47. Karlsson MO, Beal SL, Sheiner LB. Three new residual error models for population PK/PD analyses. Journal of Pharmacokinetics and Pharmacodynamics. 1995;23(6):651-72.
48. Beal SL. Ways to fit a PK model with some data below the quantification limit. Journal of pharmacokinetics and pharmacodynamics. 2001;28(5):481-504.
49. Chevance A, Jacques AM, Laurentie M, Sanders P, Henri J. The present and future of withdrawal period calculations for milk in the European Union: focus on heterogeneous, nonmonotonic data. Journal of veterinary pharmacology and therapeutics. 2017;40(3):218-30.
50. Lindbom L, Pihlgren P, Jonsson N. PsN-Toolkit—a collection of computer intensive statistical methods for non-linear mixed effect modeling using NONMEM. Computer methods and programs in biomedicine. 2005;79(3):241-57.
51. Keizer RJ, Van Benten M, Beijnen JH, Schellens JH, Huitema AD. Pirana and PCluster: a modeling environment and cluster infrastructure for NONMEM. Computer methods and programs in biomedicine. 2011;101(1):72-9.
52. Landersdorfer CB, Nguyen T-H, Lieu LT, Nguyen G, Bischof RJ, Meeusen EN, et al. Substantial Targeting Advantage Achieved by Pulmonary Administration of Colistin Methanesulfonate in a Large-Animal Model. Antimicrobial agents and chemotherapy. 2017;61(1):e01934-16.

53. Karvanen M, Malmberg C, Lagerback P, Friberg LE, Cars O. Colistin Is Extensively Lost during Standard In Vitro Experimental Conditions. Antimicrob Agents Chemother. 2017;61(11).
54. Huang JX, Blaskovich MA, Pelingon R, Ramu S, Kavanagh A, Elliott AG, et al. Mucin binding reduces colistin antimicrobial activity. Antimicrobial agents and chemotherapy. 2015;59(10):5925-31.
55. Hinderling PH. Red blood cells: a neglected compartment in pharmacokinetics and pharmacodynamics. Pharmacological reviews. 1997;49(3):279-95.
56. Azad MA, Huang JX, Cooper MA, Roberts KD, Thompson PE, Nation RL, et al. Structure–activity relationships for the binding of polymyxins with human α-1-acid glycoprotein. Biochemical pharmacology. 2012;84(3):278-91.
57. Bouchene S, Marchand S, Friberg LE, Björkman S, Couet W, Karlsson MO, editors. Whole Body Physiologically-Based Pharmacokinetic Model for Colistin and Colistimethate Sodium (CMS) in Six Different Species: Mouse, Rat, Rabbit, Baboon, Pig and Human. Journal of Pharmacokinetics and Pharmacodynamics; 2013.
58. Holford NH, Anderson BJ. Allometric size: The scientific theory and extension to normal fat mass. European Journal of Pharmaceutical Sciences. 2017.
59. Yousef JM, Chen G, Hill PA, Nation RL, Li J. Melatonin attenuates colistin-induced nephrotoxicity in rats. Antimicrobial agents and chemotherapy. 2011;55(9):4044-9.
60. Zavascki AP, Nation RL. Nephrotoxicity of polymyxins: Is there any difference between colistimethate and polymyxin B? Antimicrobial Agents and Chemotherapy. 2016.
61. Manchandani P, Zhou J, Babic JT, Ledesma KR, Truong LD, Tam VH. The role of renal drug exposure in polymyxin B-induced nephrotoxicity. Antimicrobial Agents and Chemotherapy. 2017:AAC. 02391-16.
62. Vardakas KZ, Falagas ME. Colistin versus polymyxin B for the treatment of patients with multidrug-resistant Gram-negative infections: a systematic review and meta-analysis. International Journal of Antimicrobial Agents. 2016.
63. Ordooei Javan A, Shokouhi S, Sahraei Z. A review on colistin nephrotoxicity. European journal of clinical pharmacology. 2015.
64. Li M, Gehring R, Riviere JE, Lin Z. Development and application of a population physiologically based pharmacokinetic model for penicillin G in swine and cattle for food safety assessment. Food and Chemical Toxicology. 2017;107:74-87.
65. EMA. Updated advice on the use of colistin products in animals within the European Union: development of resistance and possible impact on human and animal health. European Medicines Agency (EMA), 2016 EMA/CVMP/CHMP/231573/2016.

Legend to Figures

Figure 1: A global diagram of the physiologically based pharmacokinetic (PBPK) model of CMS and colistin in swine.

The whole body PBPK model is described (A), as well as the detailed mechanism in a generic tissue (except kidneys) (B), of the IM route (C) and of the deep compartments (D).

During model development, supplementary components were added in the final model and are represented in blue (see Results). Kidney sub-compartments and urine are detailed in Fig. 2. All estimated parameters (in italic) are detailed in Table IV.
Vtissue: tissue volume; Qtissue: blood flow; Kp_tissue: partition coefficient; IV: intravenous dose; IM: intramuscular dose

Figure 2: Schematic representation of the renal sub-compartments in the PBPK model of CMS and colistin in swine.
All estimated parameters (in italic) are detailed in Table IV.
During model development, supplementary components were added in the final model and are represented in blue (see Results).
$\mathrm{Q_{KID}}$: renal blood flow; $\mathrm{Q_{URI}}$: urinary flow; $\mathrm{Q_{TUB}}$: tubular flow; $CL_{GFR\_CMS}/CL_{GFR\_COLI}$: filtration clearance of CMS and colistin

Figure 3: Visual Predictive Checks of the PBPK model for CMS and colistin plasma concentrations after one IV (A) and one IM (B) of CMS, used for model calibration.
Plasma data come from experiment n°1 for A (125,000 UI/kg of CMS after IV infusion over 1h) and from experiment n°2 for B (125,000 UI/kg of CMS after IM injection).
Blue dots represent the observed plasma concentrations; the grey areas represent the 90% prediction interval of the model, whereas the black solid line represents the median; the purple area represents the 95% confidence interval around the median; the horizontal dashed black lines represent the LOQ. In the smaller panels, blue areas represent the simulation-based 95% confidence intervals for the fraction of model simulated samples below the LOQ (BLOQ) at each time point, whereas the blue solid line represents the actual observed fraction of BLOQ samples.

Figure 4: Visual Predictive Checks of the PBPK model for CMS and colistin plasma concentrations after a dosing scheme to achieve steady-state (A) and repeated IM administrations (B) of CMS, used for model calibration.
Plasma data come from experiment n°3 for A (75,000 UI/kg IV during 1 h; 1.5 h without administration; 50,000 UI/kg IV during 4 h) and from experiment n°4 for B (50,000 UI/kg of CMS divided in two IM injection per day).
Blue dots represent the observed plasma concentrations; the grey areas represent the 90% prediction interval of the model, whereas the black solid line represents the median; the purple area

represents the 95% confidence interval around the median; the horizontal dashed black lines represent the LOQ.
No data below LOQ (BLOQ) were observed in A. For B, fractions of BLOQ are not represented due to the sparse sampling but they are discussed in the text.

Figure 5: Visual Predictive Checks of the PBPK model for cumulative urinary quantities concentrations after one IV of CMS, used for model calibration.
Urinary data come from experiment n°1 (125,000 UI/kg of CMS after IV infusion over 1h).
Blue dots represent the observed plasma concentrations; the grey area represents the 90% prediction interval of the model, whereas the black solid line represents the median. The purple area represents the 95% confidence interval around the median;

Figure 6: Visual Predictive Checks of the PBPK model for total renal concentrations after one IV (A), the dosing scheme of infusions for steady-state (B) and repeated IM administrations (C) of CMS, used for model calibration.
Kidney data come from experiment n°1 for A (125,000 UI/kg of CMS after IV infusion over 1h); from experiment n°3 for B (75,000 UI/kg IV during 1 h; 1.5 h without administration; 50,000 UI/kg IV during 4 h, those pigs received one IV and one IM, 48h and 24h before t=0h, respectively) and from experiment n°4 for C (50,000 UI/kg of CMS divided in two IM injection per day).
Blue dots represent the observed plasma concentrations; the grey areas represent the 90% prediction interval of the model, whereas the black solid line represents the median. The purple area represents the 95% confidence interval around the median. No data were below the LOQ (0.15 µg/g).

Figure 7: VPC of the PBPK model for CMS (A) and colistin (B) plasma concentrations after 3 days of IM administrations of CMS, used for model validation.
Observed data come from an independent experiment (n°5: 50,000 UI/kg of CMS divided in two IM injection per day during 3 days) that was not used for model calibration.
Blue dots represent the observed plasma concentrations; the grey areas represent the 90% prediction interval of the model, whereas the black solid line represents the median; the purple area represents the 95% confidence interval around the median ; the horizontal dashed black lines represent the LOQs. In the smaller panels, blue areas represent the simulation-based 95% confidence intervals for the fraction of model-simulated samples below the LOQ (BLOQ) at each time point, whereas the blue solid line represents the actual observed fraction of BLOQ samples.

Figure 8: VPC of the PBPK model for total renal concentrations after 3 days of IM administrations of CMS. Observed data come from an independent experiment (n°5: 50,000 UI/kg of CMS divided in two IM injection per day) that was not used for model calibration.
Blue dots represent the observed plasma concentrations; highlighted with grey are the areas between the 5th and 95th percentiles of model simulations, whereas the black solid line represents the median. No data were below the LOQ (0.15 µg/g).

Figure 9: CMS and colistin disposition within kidneys as given by the PBPK model.
Each percentage represents the fraction of the initial dose (100%) involved in each process.
$fu_{\_CMS}$ /$fu_{\_COLI}$: unbound fraction of CMS/colistin; GFR: glomerular filtration rate

Figure 10: Withdrawal period estimation in a 50-kg pig.
Model simulation in kidney after 3 consecutive days of CMS IM injections (50,000 UI/kg of CMS divided in two injections per day) for 1000 virtual pigs of 50 kg.
The grey area includes the 1st and 99th percentiles of model simulations, whereas the black solid line represents the median; the horizontal dashed black line represents the kidney MRL for colistin (0.20 µg/g).
WP: withdrawal period, rounded to the next whole day

TABLES

Table I: Summary of pharmacokinetic experimental studies of CMS and colistin in swine used for calibration and validation of the PBPK model

Modelling purpose	**N° of experiment**	**Route**	**Dose of CMS (UI/kg)**	**Number of pigs**	**Number of doses**	**Numbers of samples per pig (min-max)**
CALIBRATION	1	IV	**125,000** (1 h- infusion)	10	1	Blood: 12 Urine: (2-9) Kidneys: 1
	2	IM	**125,000**	6	1	Blood: 12
	3	IV	**75,000** during 1 h; 1.5 h without administration; **50,000** during 4 h	6	1	Blood: (1-4) All organs: 1
	4	IM	**50,000** (divided in two administrations of 2 per day)	15	7 maximum (*i.e.* 14 injections)	Blood: (1-4) Kidneys: 1
VALIDATION	5	IM	**50,000** (divided in two administrations of 2 per day)	20	3 (*i.e.* 6 injections)	Blood: 1 Kidneys, fat, skin, liver, muscles: 1

Notes: The abbreviations for the route: IM, intramuscular injection; IV, intravenous injection. Some pigs were used in different experiments (n°1, 2 and 3) in model calibration.

Table II: physiological and *chemical*-specific parameters for PBPK model

Compartments	**Volume (fraction of BW)**	**References**	**Blood flow (fraction of CO)**	**References**
Arterial blood	0.027	(28, 41)	1	-
Venous blood	0.053	(28, 41)	1	-
Lung	0.027	(35)	1	-
Brain	0.0034	(31, 39, 41)	0.02	(39, 40)
Heart	0.0062	(31, 41)	0.037	(29, 30)
Muscles	0.38	(31, 40)	0.2	(34, 40, 41)
Skin	0.077	(31, 41)	0.05	(37)
Adipose	0.18	(31, 41)	0.17	(34, 40)
GIT	0.062	(31, 39, 40)	0.22	(38, 39)
Liver	0.027	(31, 39, 41)	Hepatic artery + GIT blood flow : 0.27	(34, 38, 39)
Kidneys	0.0048	(31, 41)	0.13	(38-40)
Vascular	0.067 [a]	(27, 29)	-	-
Extravascular	0.12 [a]	(30)	-	-
Tubular lumen	0.2 [a,b]	(36)	-	-
Intracellular	0.613 [a,c]		-	-
Bladder	0.01 [d]	-	-	-
Rest of Body	0.14 [e]	-	0.12 [f]	-
TOTAL	*1*	-	*1*	-

Other parameters (units)	**Value**	**References**
Cardiac output[g] (L/h/kg)	8.5	(27, 39, 40)
Haematocrit	0.40	(42)
GFR (L/h/kg)	0.074	(32, 33)
Urinary flow (L/h/kg)	0.0022	Experimental data
Tubular flow (L/h/kg)	67% of GFR	(36)

Colistin partition coefficient (Kp)	**Mean value +/- SD (unitless)**	**References**
Lung	0.73 ± 0.31	Experimental data
Brain	0.71 ± 0.37	
Heart	0.29 ± 0.14	
Muscles	0.10 ± 0.029	
Skin	0.43 ± 0.17	
Adipose	0.25 ± 0.11	
GIT	0.41 ± 0.17	
Liver	0.52 ± 0.26	
Kidneys	NC	-
Rest of body	0.4	Fixed to the mean of others Kps
Unbound fraction CMS	0.37	Experimental data (see Table III)
Unbound fraction colistin	0.40	(25)

[a] defined as fraction of kidney volume; [b] fixed to human value; [c] calculated by subtracting all fractions of the 3 other sub-compartments; [d] arbitrary fixed; [e] calculated by subtracting all fractions of the other organs; [f] calculated by subtracting all fractions of the other organs except arteries, veins and lung; [g] Cardiac output was multiplied by (1 – haematocrit) to get the total plasmatic flow

NC : not concerned ; GFR : glomerular filtration rate ; GIT : gastro-intestinal tract

Table III: Results of experiments for the determination of plasmatic unbound fraction of CMS in pigs (n=3)

Theoretical CMS concentration in parent solution (µg/mL)	**Media**	**Measured CMS concentration in parent solution (µg/mL)**	**CMS concentration in ultratfiltrate (µg/mL)**	**Fraction of loss**	**Unbound fraction**
5	Phosphate buffer	6.3	4.5 ± 0,5	28%	NC
5	Pig plasma	4.4	1.2 ± 0.12	73%	0.38 ± 0.04[a]
0.5		0.49	0.12 ± 0.01	75%	0.36 ± 0.02[a]

[a]: Calculated accounting for the loss due to the CMS degradation (hydrolysis) and the non-specific binding to the tube determined in phosphate buffer; NC : not concerned

Table IV: CMS and colistin parameters optimised in the PBPK model

Parameters (unit)	Value *[CI 95%]*	IIV *[CI 95%]*	Meaning
CMS			
K_{hyd_CMS} (h^{-1})	0.262 *[0.238-0.290]*	-	CMS hydrolysis constant (common for all compartments)
K_{IM_CMS} (h^{-1})	1.78 *[1.39-2.35]*	-	Absorption constant of CMS for intra-muscular route
Kp_{mix_CMS} (unitless)	0.217 *[0.189-0.242]*	-	Kp of CMS compartments (common for all compartments)
CL_{sec_CMS} ($L.h^{-1}$)	8.39 *[6.53-10.94]*	0.193 (43.5%) *[0.0840-0.403]*	Tubular CMS secretion from kidney vascular space to tubular lumen
Colistin			
K_{deg_COLI} (h^{-1})	0.389 *[0.334-0.456]*	0.0737 (26.6%) *[0.0437-0.139]*	Colistin non-renal eliminating constant (common for all compartments)
K_{IM_COLI} (h^{-1})	5.99 *[3.09-13.77]*	-	Absorption constant of colistin for intra-muscular route
K_{DEEP_COLI} (h^{-1})	0.187 *[0.135-0.295]*	-	Transfer constant of colistin from vascular compartments towards deep compartment
$K_{DEEP\_OUT\_COLI}$ (h^{-1})	0.104 *[0.0670-0.149]*	-	Transfer constant of colistin from deep compartment towards vascular compartments
K_{ON_COLI} (h^{-1})	0.0910 *[0.0524-0.157]*	-	"Binding" constant of colistin in kidney intracellular compartments
K_{OFF_COLI} (h^{-1})	0.0145 *[0.0051-0.0230]*	-	"Unbinding" constant of colistin in kidney intracellular compartments
CL_{reabs_COLI} ($L.h^{-1}$)	106 (fixed)	-	Reabsorption of colistin tubular lumen into intracellular compartment
Residual errors (proportional)			
RV_{plas_CMS}	0.171 (41 %) *[0.136-0.225]*	-	Proportional residual error for plasmatic CMS concentrations
RV_{plas_COLI}	0.166 (41 %) *[0.136-0.205]*	-	Proportional residual error for plasmatic colistin concentrations
Common RV term of CMS and colistin in plasma	0.0824 [*0.0541-0.116]*	-	L2 data item method
RV_{tissue_CMS}	0.111 (33 %) *[0.0644-0.192]*	-	Proportional residual error for the tissue CMS concentrations
RV_{KID}	0.331 (57 %) *[0.193-0.574]*	-	Proportional residual error for kidney total concentrations
RV_{URINE}	0.258 (51 %) *[0.171-0.402]*	-	Proportional residual error for urinary total concentrations

IIV: inter-individual variability; CI: confidence interval

Table V: Results of the local sensitivity analysis

Estimated parameters	Impact of a +10% in value on output[a] (in % of variation)	Impact of a -10% in value on output[a] (in % of variation)
CMS		
K_{hyd_CMS}	1.09	0.67
K_{IM_CMS}	0.22	0.40
Kp_{mix_CMS}	0.54	0.44
CL_{sec_CMS}	0.54	0.66
Colistin		
K_{deg_COLI}	**4.59**	**5.45**
K_{IM_COLI}	< 0.1	< 0.1
K_{BIND_COLI}	< 0.1	< 0.1
$K_{BIND\_OUT\_COLI}$	< 0.1	< 0.1
K_{ON_COLI}	**2.95**	**3.50**
K_{OFF_COLI}	**8.29**	**9.05**
CL_{reabs_COLI}	< 0.1	< 0.1

[a]The output is the time when the median model prediction of the kidney concentration crossed the corresponding MRL. In bold are the parameters that are the most influential for output. All parameters are detailed in Table IV.

Fig. 1

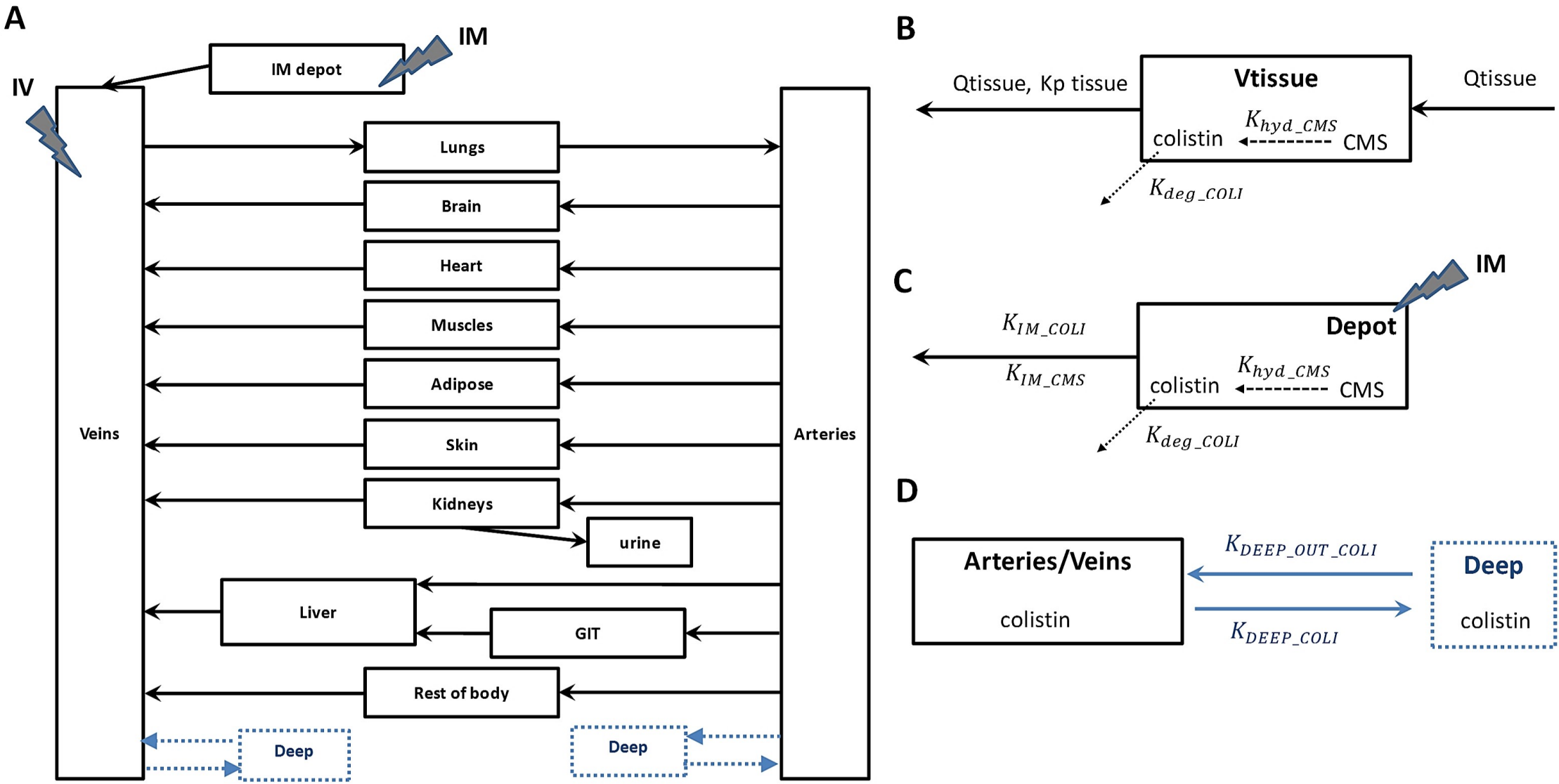
A
IM
IV
IM depot
Lungs
Brain
Heart
Muscles
Adipose
Skin
Kidneys
urine
Liver
GIT
Rest of body
Deep
Deep
Veins
Arteries
B
Qtissue, Kp tissue
Vtissue
Qtissue
colistin
K_{hyd_CMS}
CMS
K_{deg_COLI}
C
IM
K_{IM_COLI}
K_{IM_CMS}
Depot
colistin
K_{hyd_CMS}
CMS
K_{deg_COLI}
D
Arteries/Veins
colistin
$K_{DEEP\_OUT\_COLI}$
K_{DEEP_COLI}
Deep
colistin

Fig. 2

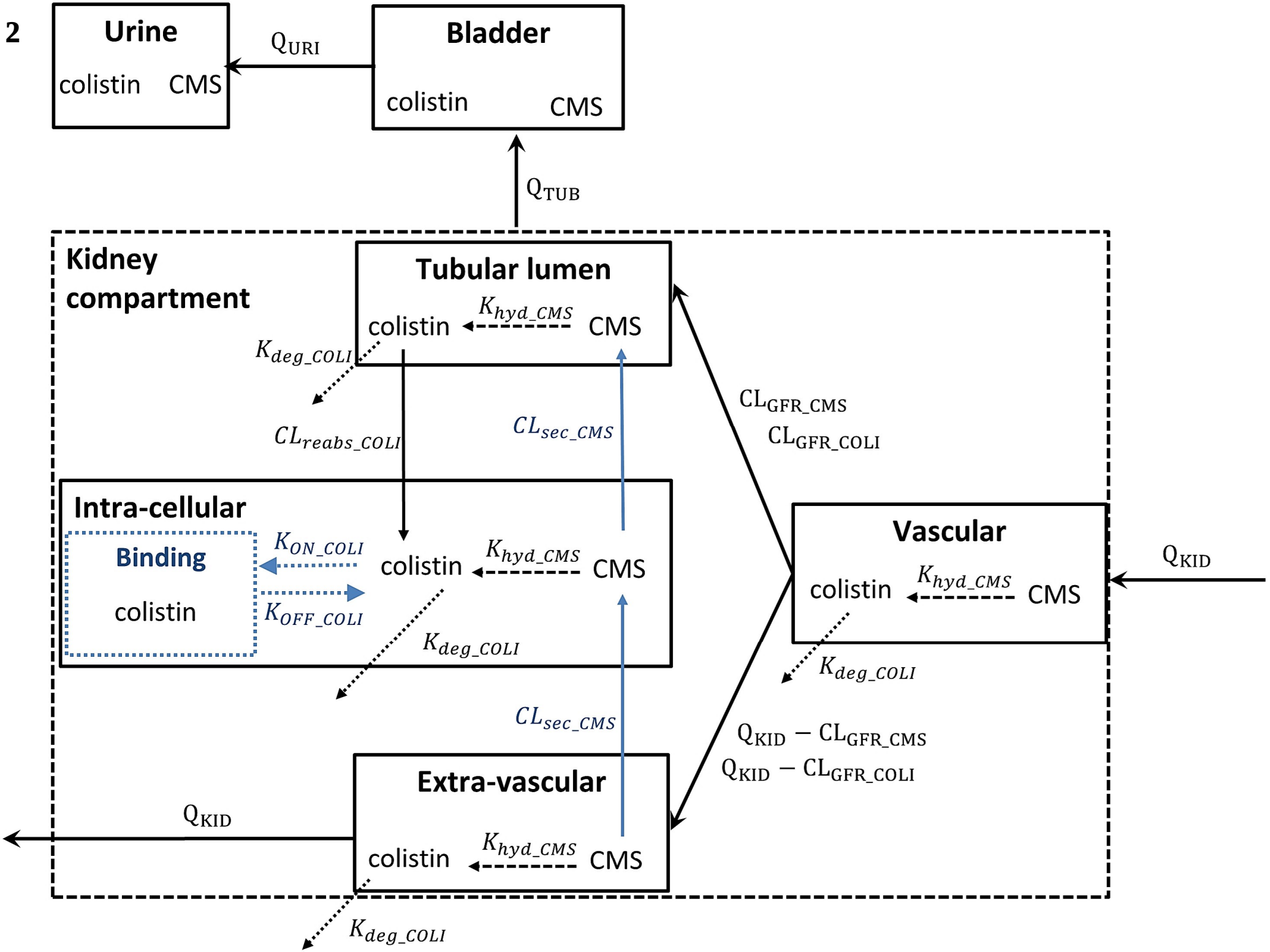
Urine
colistin
CMS
Q_{URI}
Bladder
colistin
CMS
Q_{TUB}
Kidney compartment
Tubular lumen
colistin
K_{hyd_CMS}
CMS
K_{deg_COLI}
CL_{reabs_COLI}
CL_{sec_CMS}
CL_{GFR_CMS}
CL_{GFR_COLI}
Intra-cellular
Binding
colistin
K_{ON_COLI}
K_{OFF_COLI}
colistin
K_{hyd_CMS}
CMS
K_{deg_COLI}
Vascular
colistin
K_{hyd_CMS}
CMS
Q_{KID}
K_{deg_COLI}
CL_{sec_CMS}
$Q_{KID} - CL_{GFR\_CMS}$
$Q_{KID} - CL_{GFR\_COLI}$
Extra-vascular
colistin
K_{hyd_CMS}
CMS
Q_{KID}
K_{deg_COLI}

Fig. 3

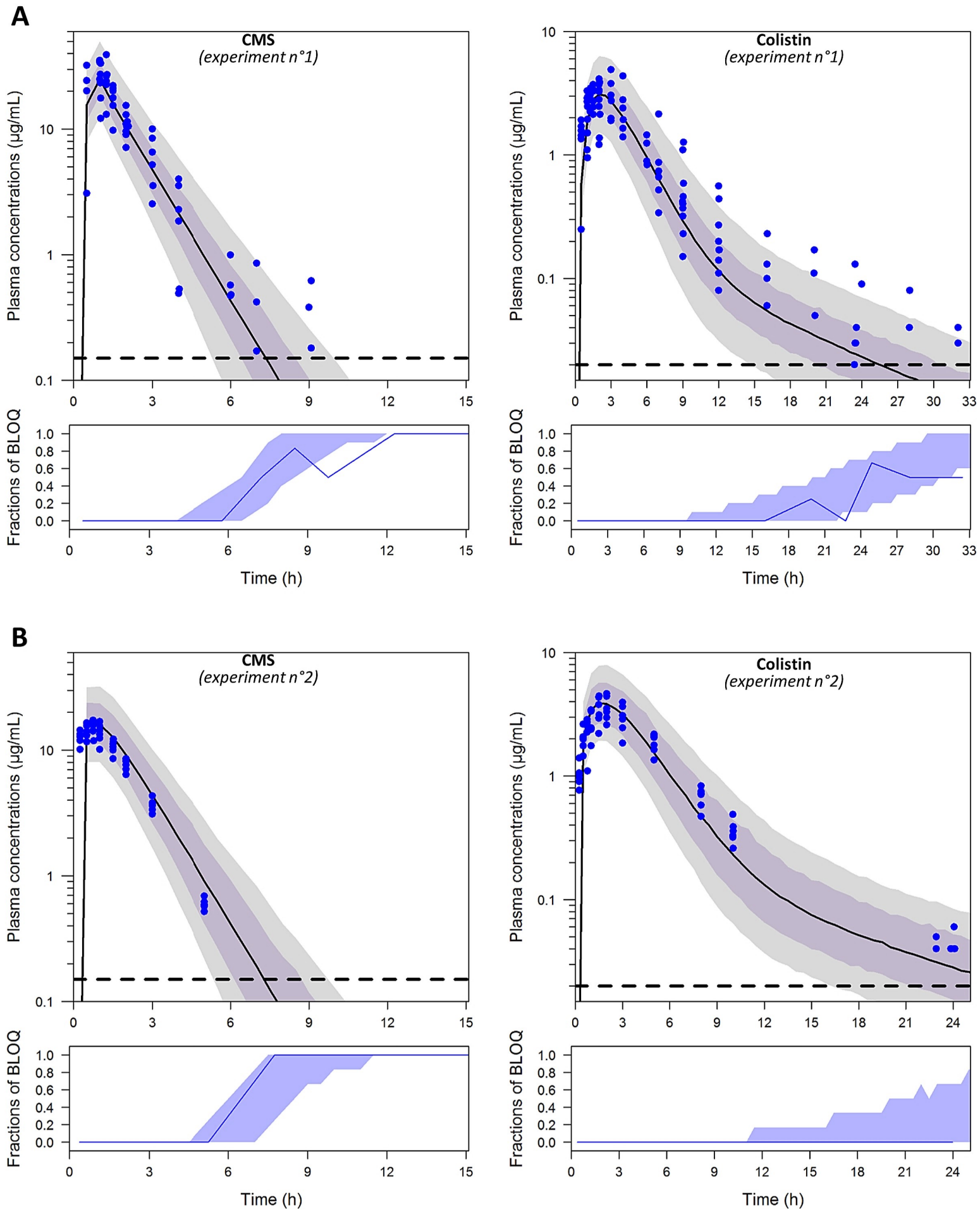
A
CMS
(experiment n°1)
Colistin
(experiment n°1)
Plasma concentrations (µg/mL)
Fractions of BLOQ
Time (h)
B
CMS
(experiment n°2)
Colistin
(experiment n°2)
Plasma concentrations (µg/mL)
Fractions of BLOQ
Time (h)

Fig. 4

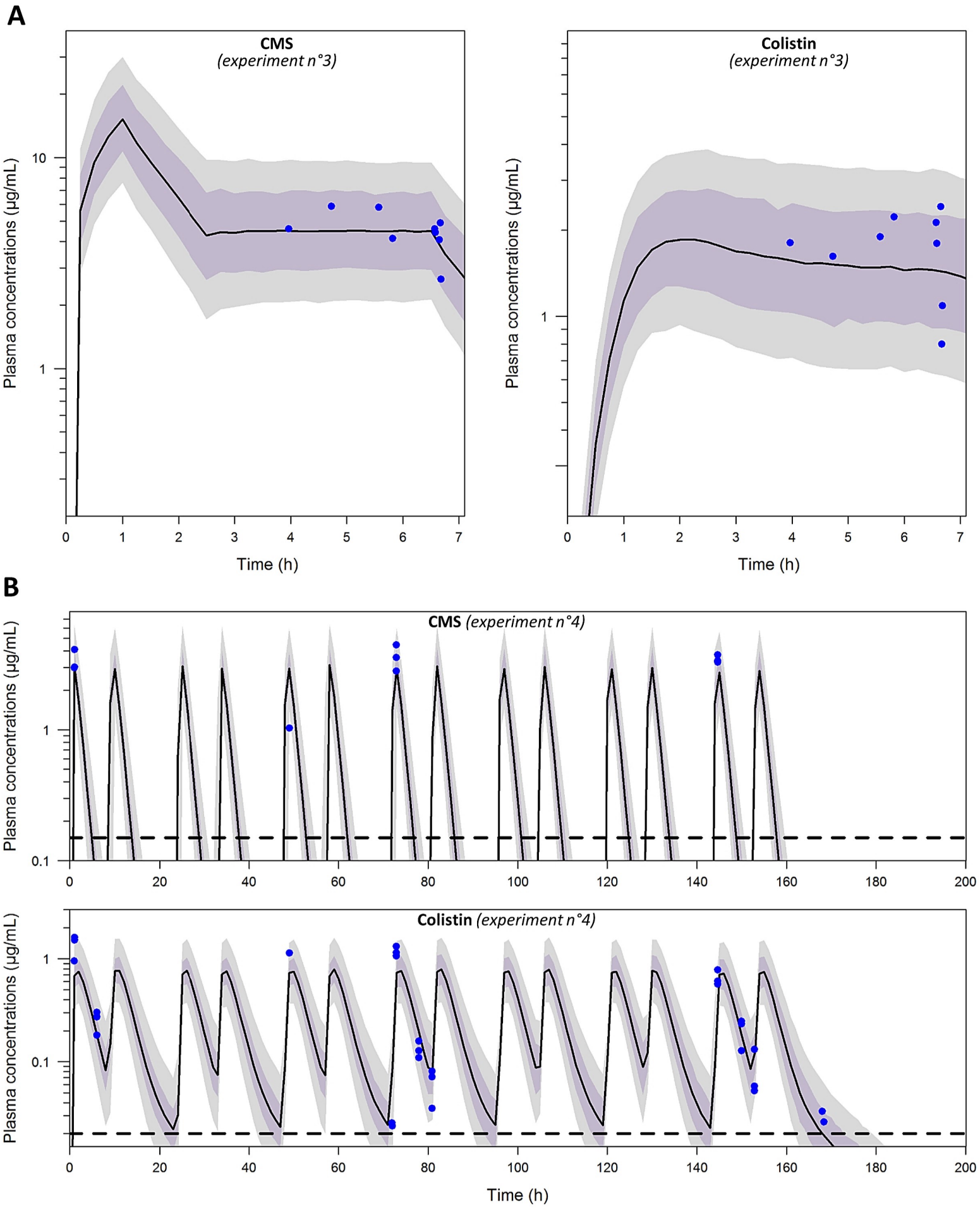
A
CMS
(experiment n°3)
Colistin
(experiment n°3)
Plasma concentrations (µg/mL)
Time (h)
B
CMS (experiment n°4)
Colistin (experiment n°4)
Plasma concentrations (µg/mL)
Time (h)

Fig. 5

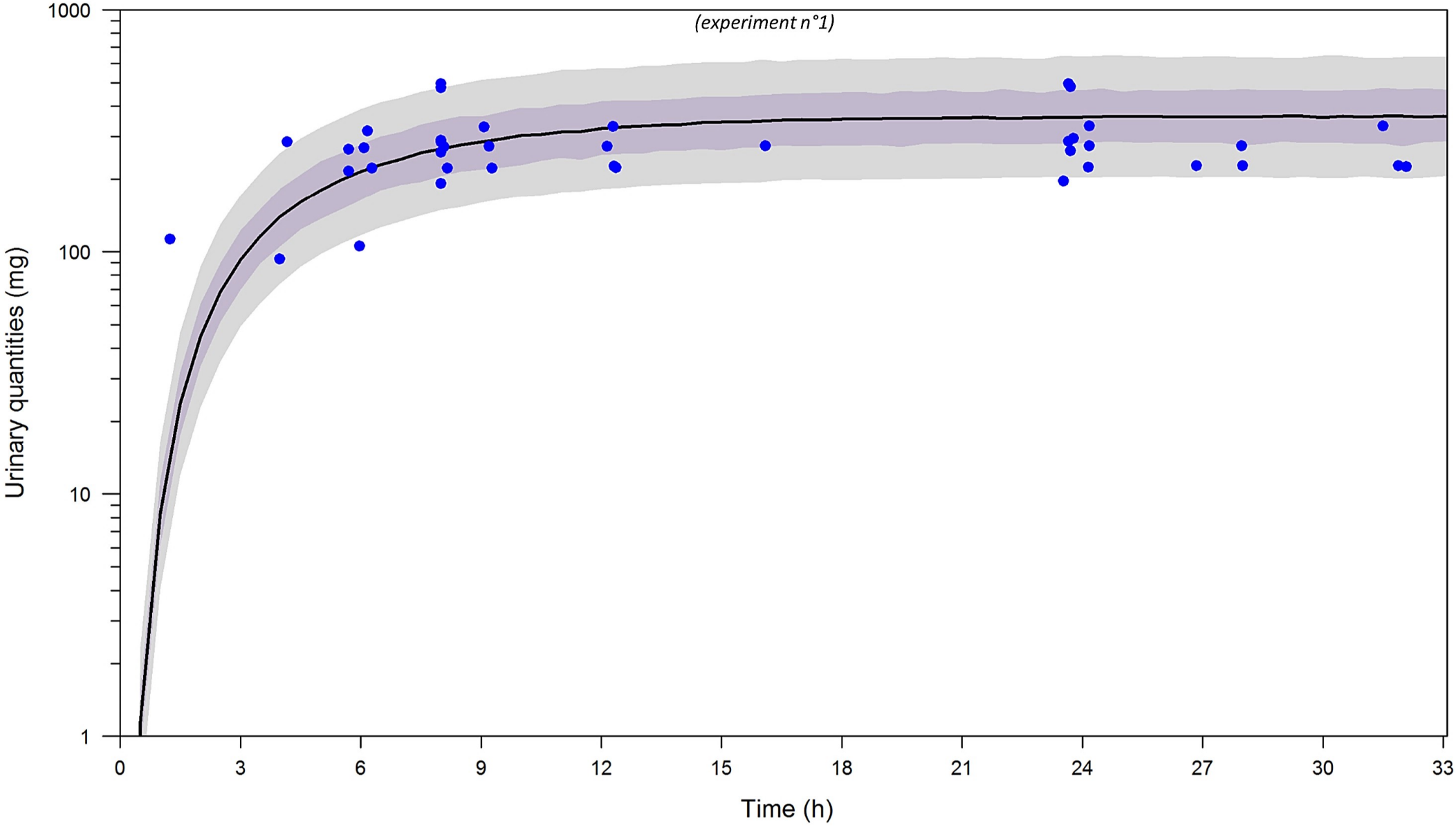
(experiment n°1)
Urinary quantities (mg)
1000
100
10
1
0
3
6
9
12
15
18
21
24
27
30
33
Time (h)

Fig. 6

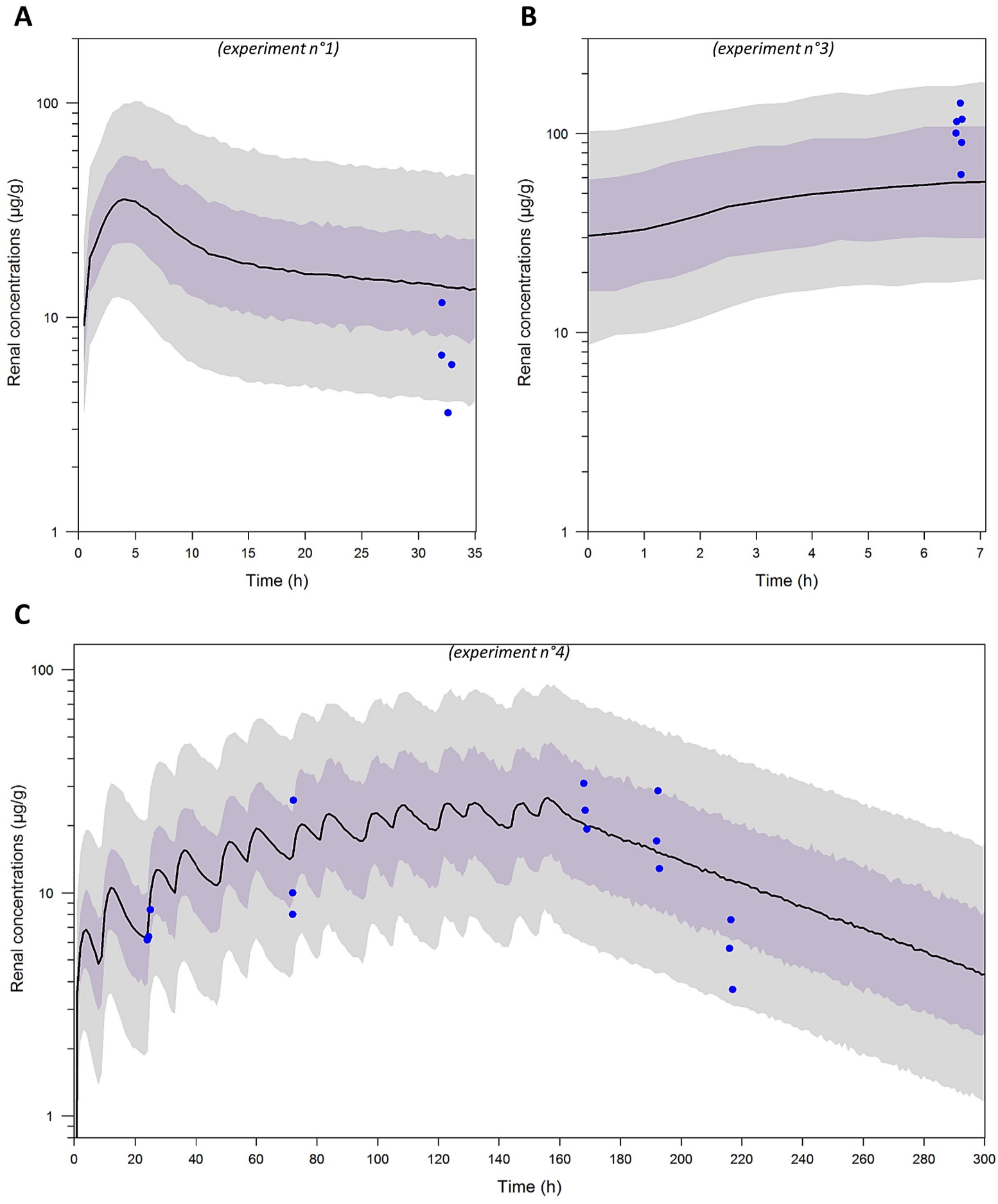
A
(experiment n°1)
Renal concentrations (µg/g)
100
10
1
0
5
10
15
20
25
30
35
Time (h)
B
(experiment n°3)
Renal concentrations (µg/g)
100
10
1
0
1
2
3
4
5
6
7
Time (h)
C
(experiment n°4)
Renal concentrations (µg/g)
100
10
1
0
20
40
60
80
100
120
140
160
180
200
220
240
260
280
300
Time (h)

Fig. 7

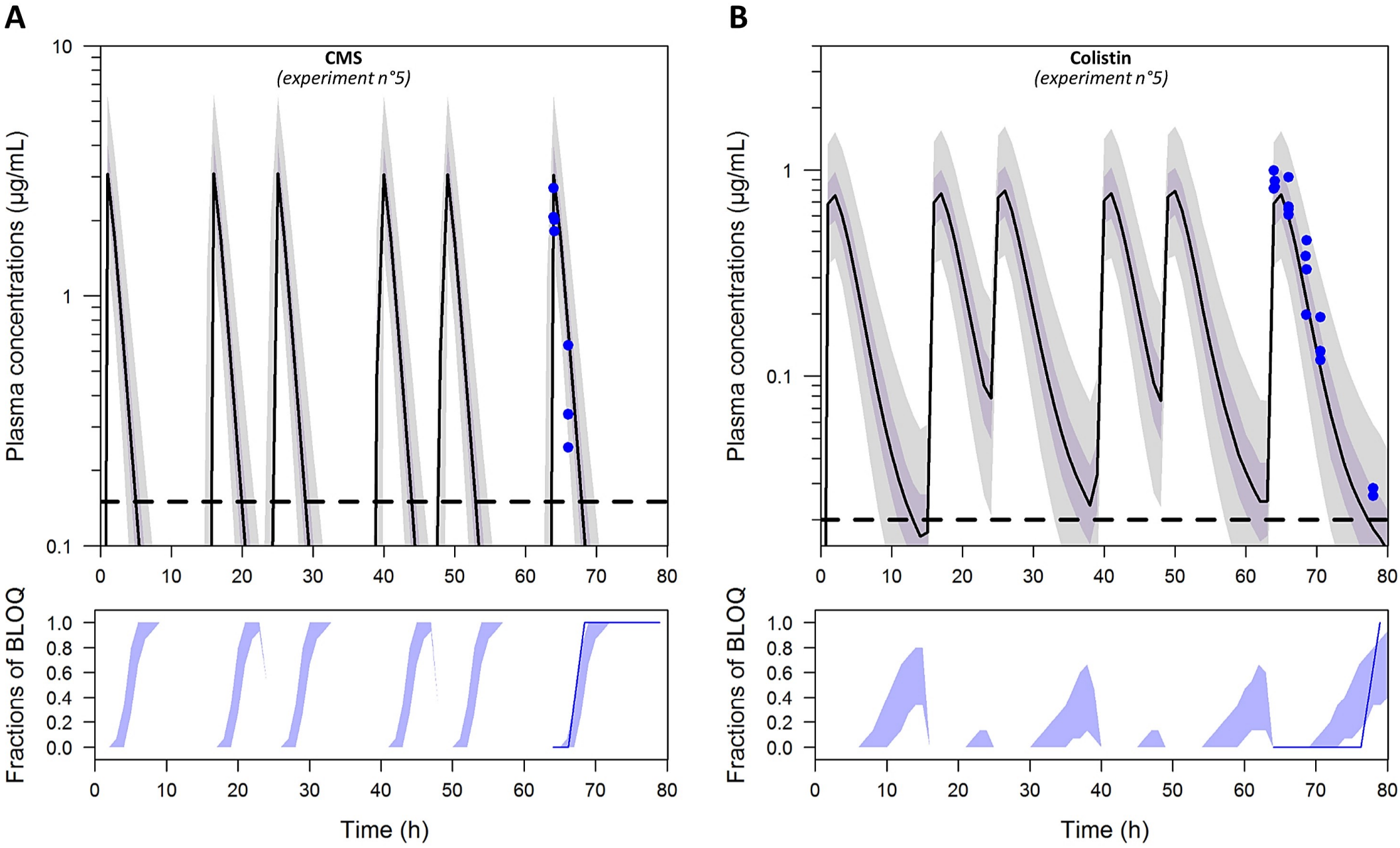
A
CMS
(experiment n°5)
Plasma concentrations (µg/mL)
10
1
0.1
0
10
20
30
40
50
60
70
80
Fractions of BLOQ
1.0
0.8
0.6
0.4
0.2
0.0
Time (h)
B
Colistin
(experiment n°5)
Plasma concentrations (µg/mL)
1
0.1
Fractions of BLOQ
Time (h)

Fig. 8

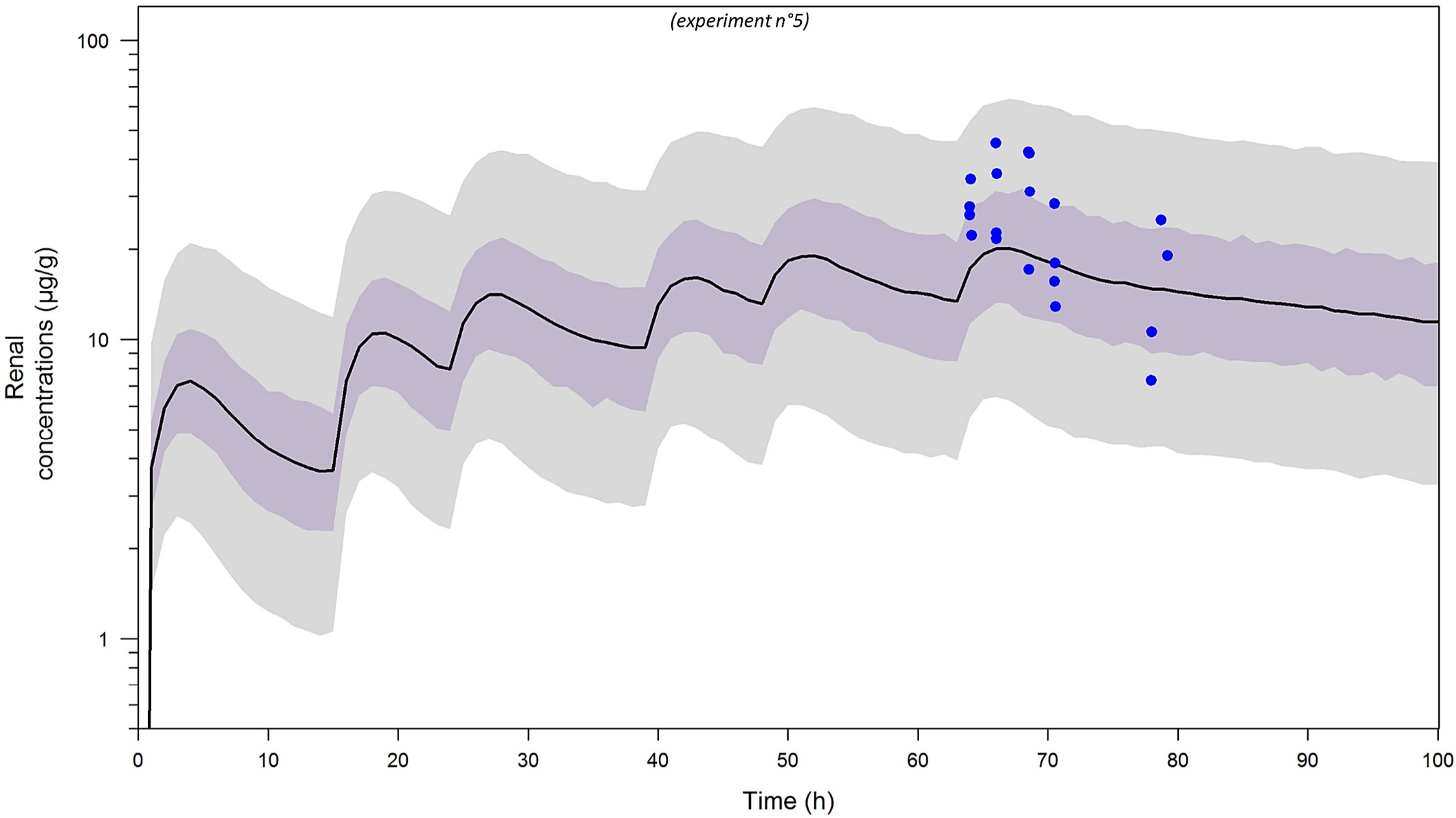
(experiment n°5)
Renal concentrations (µg/g)
100
10
1
0
10
20
30
40
50
60
70
80
90
100
Time (h)

Fig. 9

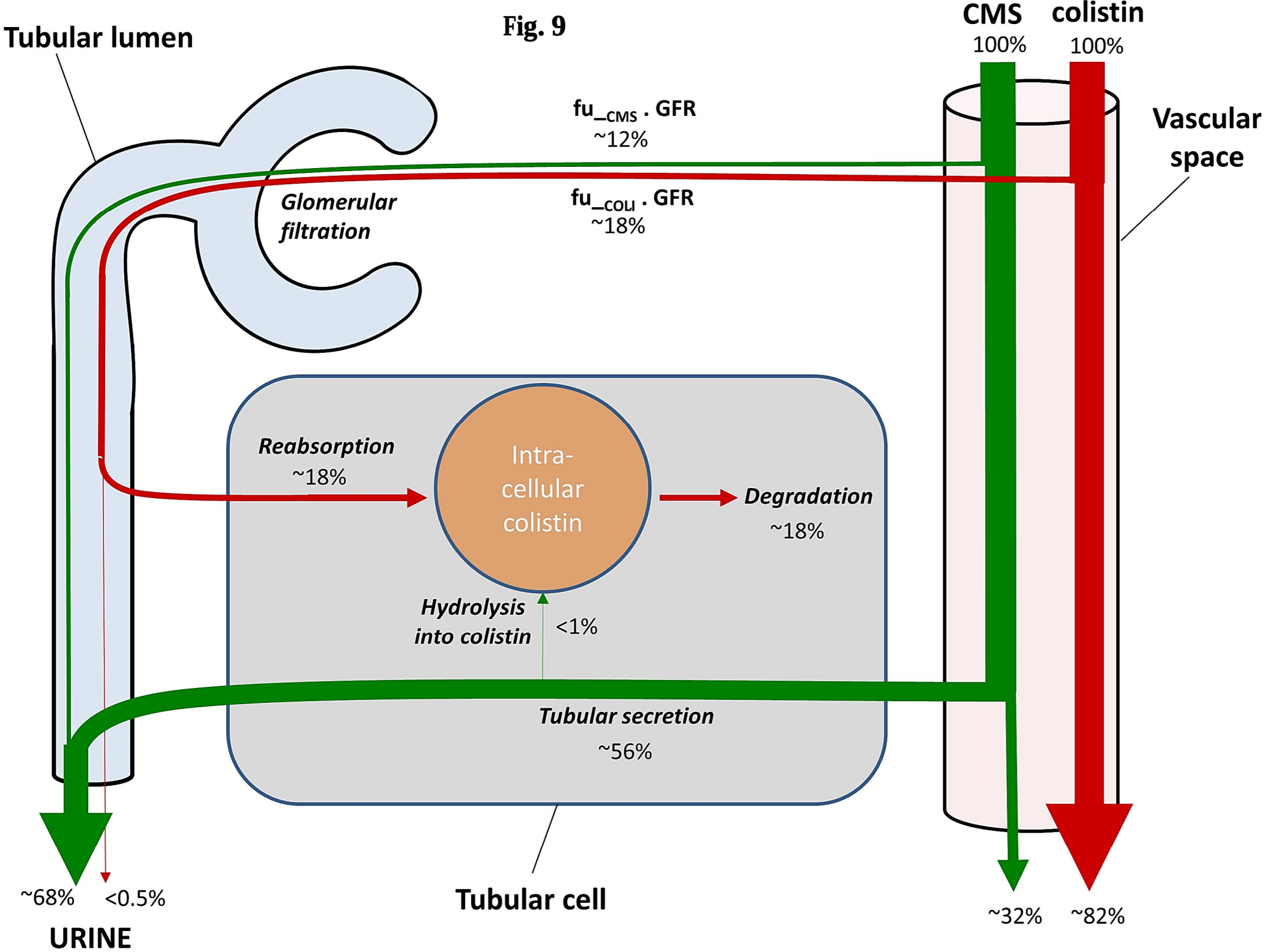
Tubular lumen
CMS
100%
colistin
100%
Vascular space
fu_CMS . GFR
~12%
Glomerular filtration
fu_COLI . GFR
~18%
Reabsorption
~18%
Intra-cellular colistin
Degradation
~18%
Hydrolysis into colistin
<1%
Tubular secretion
~56%
~68%
<0.5%
URINE
Tubular cell
~32%
~82%

Fig. 10

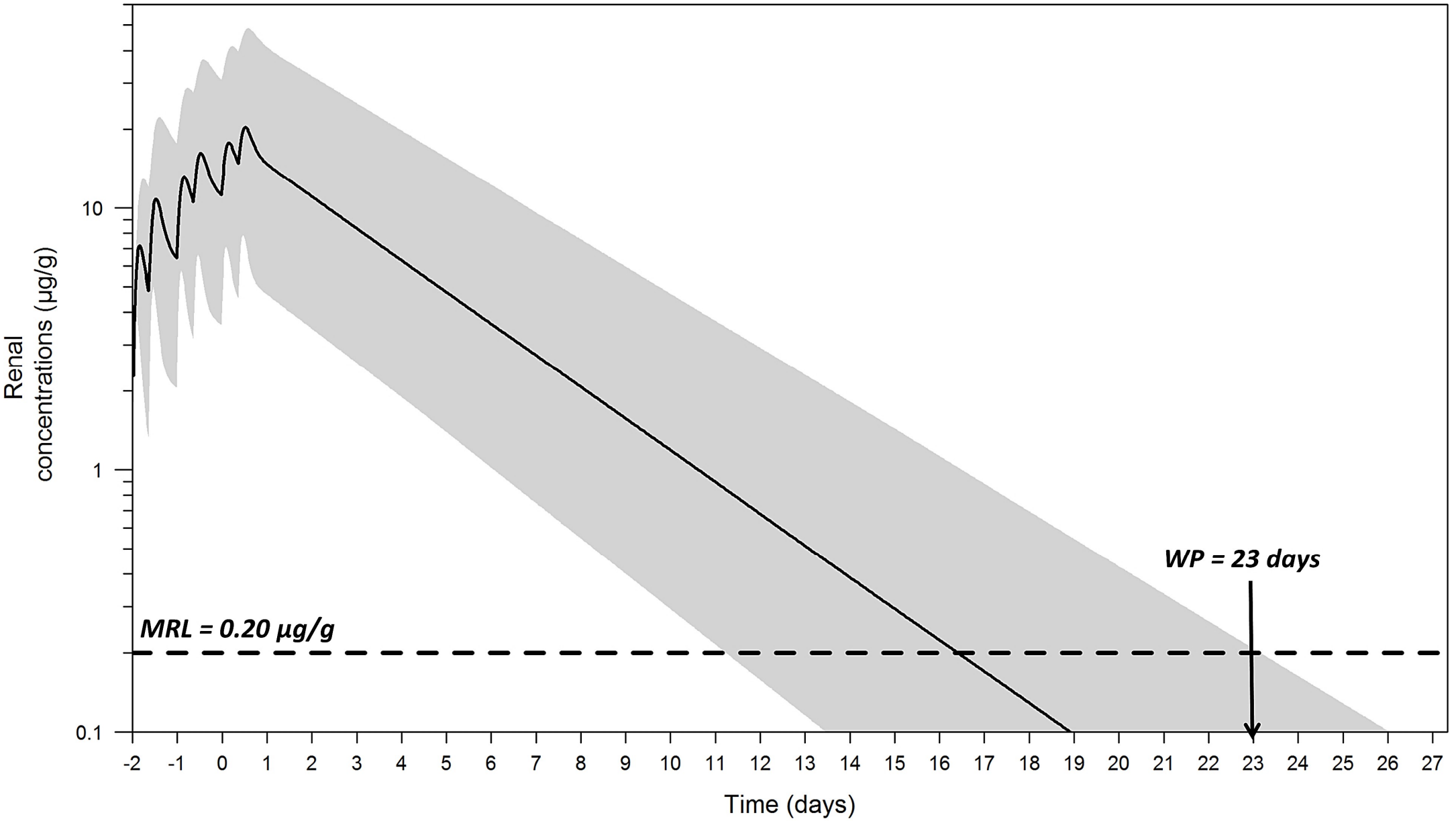
Renal concentrations (µg/g)
10
1
0.1
MRL = 0.20 µg/g
WP = 23 days
-2 -1 0 1 2 3 4 5 6 7 8 9 10 11 12 13 14 15 16 17 18 19 20 21 22 23 24 25 26 27
Time (days)

Supplementary figures legend

Figure S1: Goodness-of-fit plots for model validation
Population predicted (PRED) versus observed concentrations or quantities (DV) in log-log scale (A) and linear scale (B).
Individual predicted (PRED) versus observed concentrations or quantities (DV) in log-log scale (C) and linear scale (D).

Figure S2: Visual Predictive Checks of the PBPK model for colistin tissue data in liver (A), muscles (B), skin (C), fat (D), used for model validation.
Observed data come from an independent experiment (n°5: 50,000 UI/kg of CMS divided in two IM injection per day during 3 days) that was not used for model calibration.
Blue dots represent the observed tissue concentrations; highlighted with grey are the areas between the 5th and 95th percentiles of model simulations, whereas the black solid line represents the median; the purple area represents the 95% confidence interval around the median; the horizontal dashed black line represents the LOQ. In the lower panels, blue areas represent the simulation-based 95% confidence intervals for the fraction of data below the LOQ (BLOQ), whereas the blue solid line represents the actual observed fraction of BLOQ samples.

Figure S3: Visual Predictive Checks of the PBPK model for CMS tissue data in liver (A), muscles (B), skin (C), fat (D), used for model validation.
Observed data come from an independent experiment (n°5: 50,000 UI/kg of CMS divided in two IM injection per day during 3 days) that was not used for model calibration.
Blue dots represent the observed tissue concentrations; highlighted with grey are the areas between the 5th and 95th percentiles of model simulations, whereas the black solid line represents the median; the purple area represents the 95% confidence interval around the median; the horizontal dashed black line represents the limit of quantification. In the lower panels, blue areas represent the simulation-based 95% confidence intervals for the fraction of data below the LOQ (BLOQ), whereas the blue solid line represents the actual observed fraction of BLOQ samples.

Figure S4: Relative contribution of CMS and colistin in total kidney concentrations.

CMS concentrations (green), colistin concentrations (red) and total concentrations in kidney after one IV of CMS (10 mg/kg) for a 50-kg pig.

Figure S5: Evolution of the mass balance predicted by the model after one IV of CMS, as expressed in relative quantities for CMS (A) and colistin (B) in each compartment.
GIT : gastro-intestinal tract

Figure S6: Withdrawal period estimation in a 100-kg pig
Model simulation in kidney after 3 consecutive days of CMS IM injections (50,000 UI/kg of CMS divided in two injections per day) for 1000 virtual pigs of 100 kg.
The grey area includes the 1st and 99th percentiles of model simulations, whereas the black solid line represents the median; the horizontal dashed black line represents the kidney MRL (0.20 µg/g).
WP: withdrawal period, rounded to the next whole day

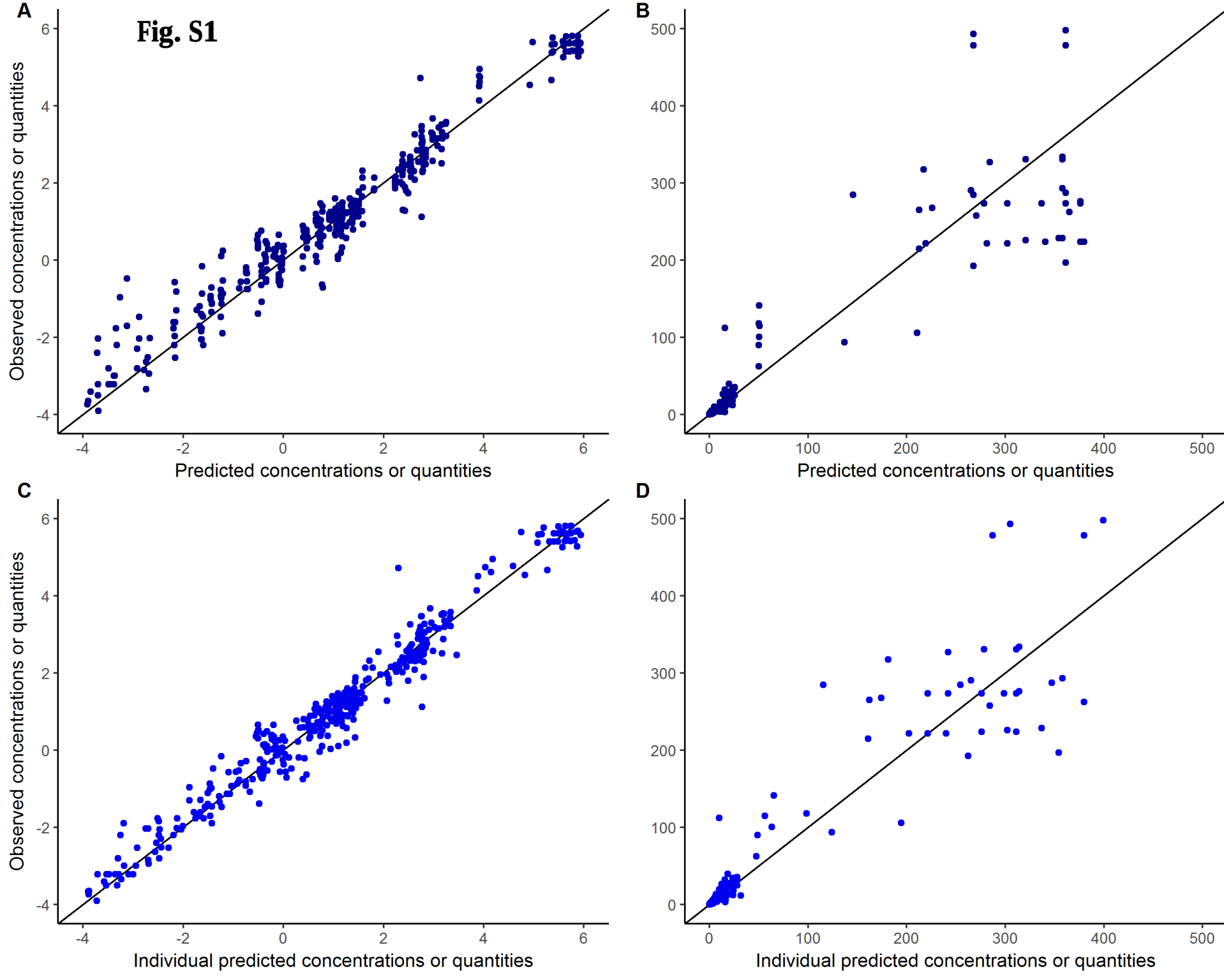
Fig. S1
A
B
C
D
Observed concentrations or quantities
Predicted concentrations or quantities
Individual predicted concentrations or quantities
-4
-2
0
2
4
6
0
100
200
300
400
500

Fig. S2

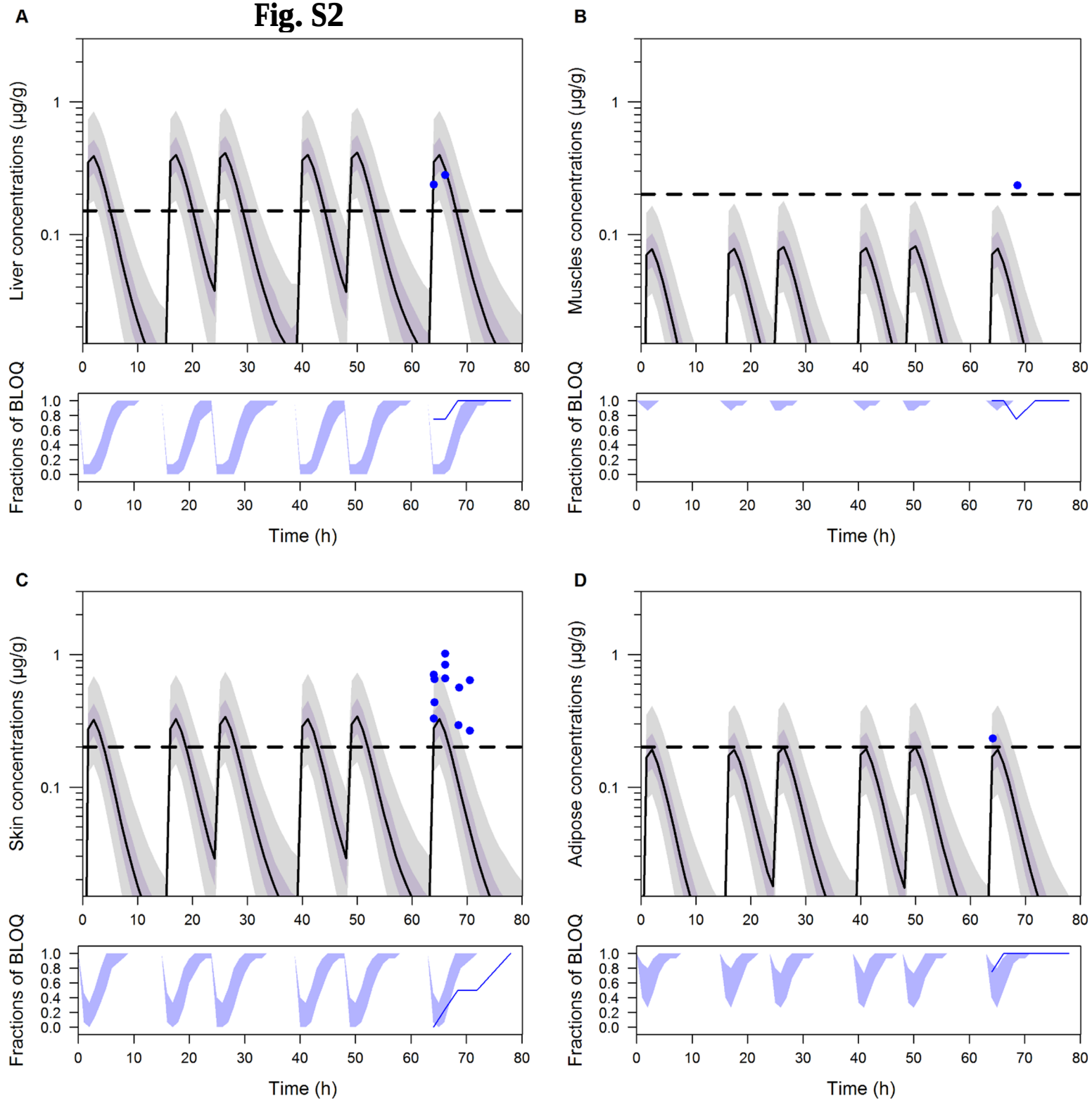
A
Liver concentrations (µg/g)
1
0.1
0 10 20 30 40 50 60 70 80
Fractions of BLOQ
1.0 0.8 0.6 0.4 0.2 0.0
0 10 20 30 40 50 60 70 80
Time (h)
B
Muscles concentrations (µg/g)
1
0.1
0 10 20 30 40 50 60 70 80
Fractions of BLOQ
1.0 0.8 0.6 0.4 0.2 0.0
0 10 20 30 40 50 60 70 80
Time (h)
C
Skin concentrations (µg/g)
1
0.1
0 10 20 30 40 50 60 70 80
Fractions of BLOQ
1.0 0.8 0.6 0.4 0.2 0.0
0 10 20 30 40 50 60 70 80
Time (h)
D
Adipose concentrations (µg/g)
1
0.1
0 10 20 30 40 50 60 70 80
Fractions of BLOQ
1.0 0.8 0.6 0.4 0.2 0.0
0 10 20 30 40 50 60 70 80
Time (h)

Fig. S3

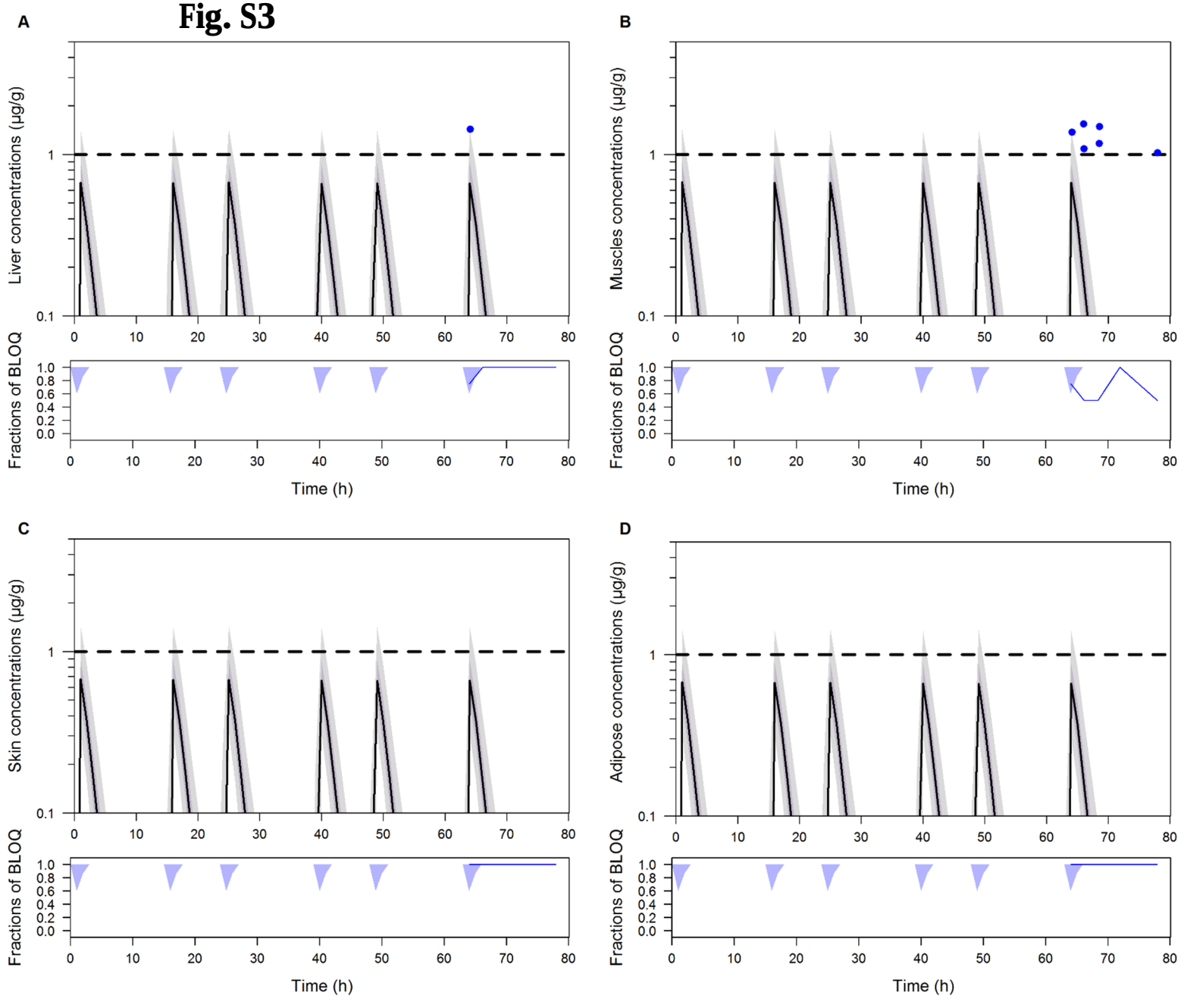
A
Liver concentrations (µg/g)
1
0.1
0 10 20 30 40 50 60 70 80
Fractions of BLOQ
1.0 0.8 0.6 0.4 0.2 0.0
0 10 20 30 40 50 60 70 80
Time (h)
B
Muscles concentrations (µg/g)
1
0.1
0 10 20 30 40 50 60 70 80
Fractions of BLOQ
1.0 0.8 0.6 0.4 0.2 0.0
0 10 20 30 40 50 60 70 80
Time (h)
C
Skin concentrations (µg/g)
1
0.1
0 10 20 30 40 50 60 70 80
Fractions of BLOQ
1.0 0.8 0.6 0.4 0.2 0.0
0 10 20 30 40 50 60 70 80
Time (h)
D
Adipose concentrations (µg/g)
1
0.1
0 10 20 30 40 50 60 70 80
Fractions of BLOQ
1.0 0.8 0.6 0.4 0.2 0.0
0 10 20 30 40 50 60 70 80
Time (h)

Fig. S4

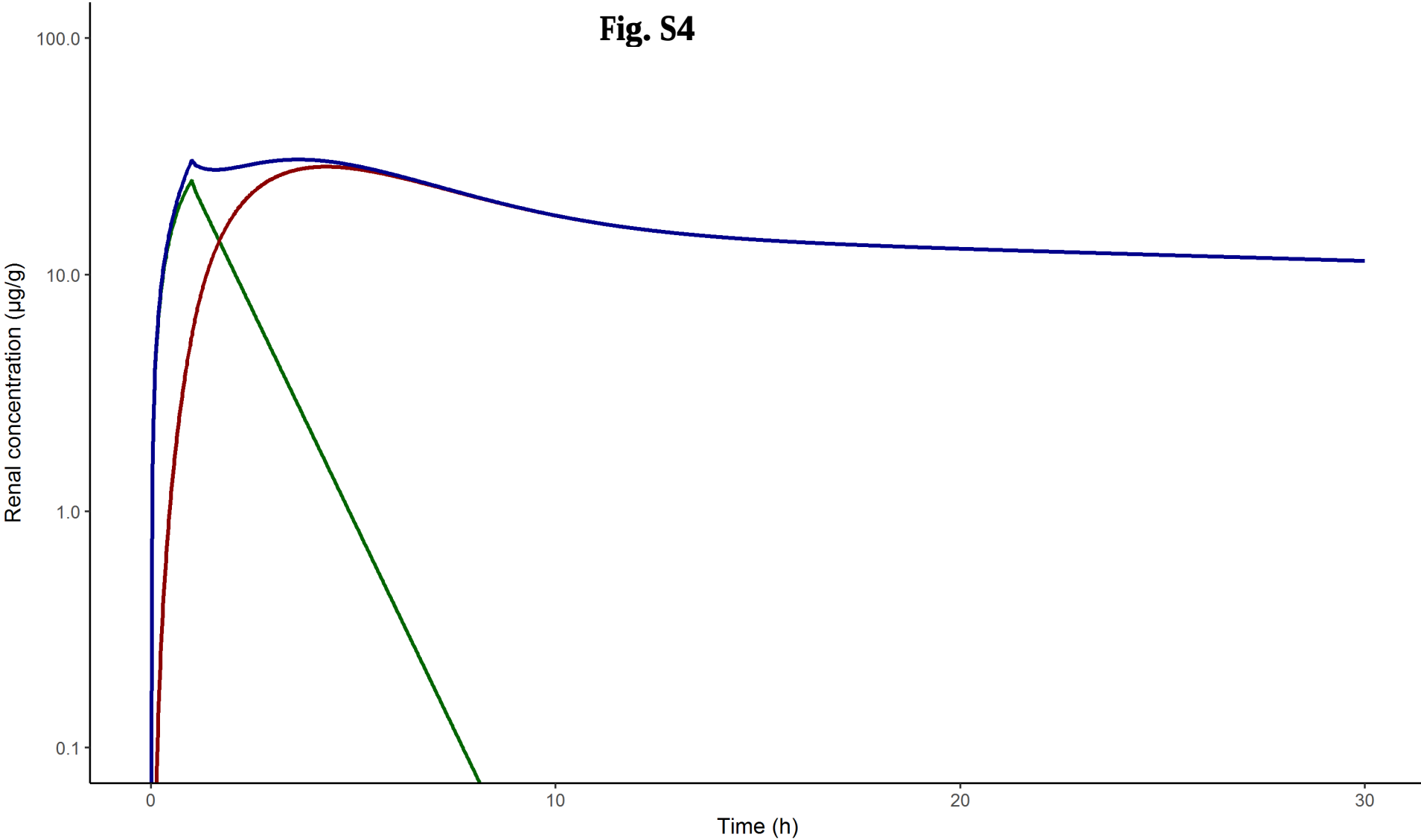

Fig. S5

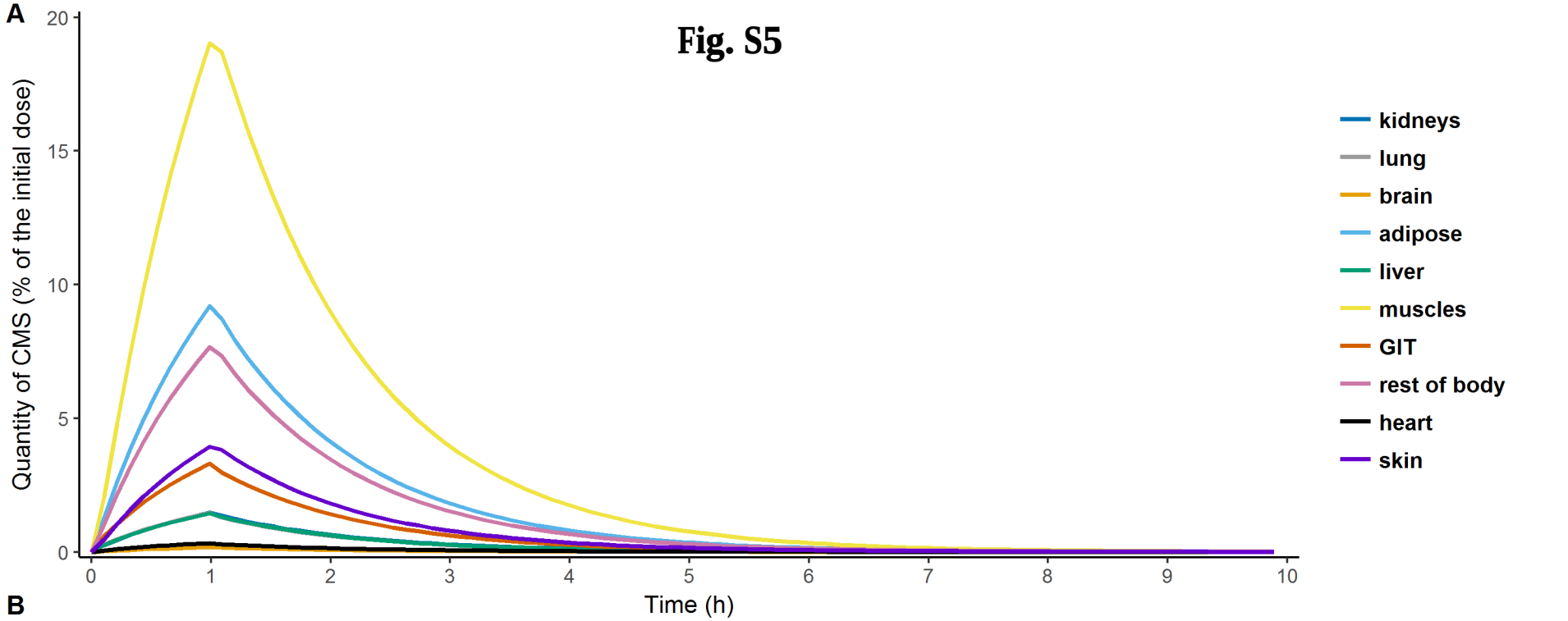
A
Quantity of CMS (% of the initial dose)
Time (h)
kidneys
lung
brain
adipose
liver
muscles
GIT
rest of body
heart
skin

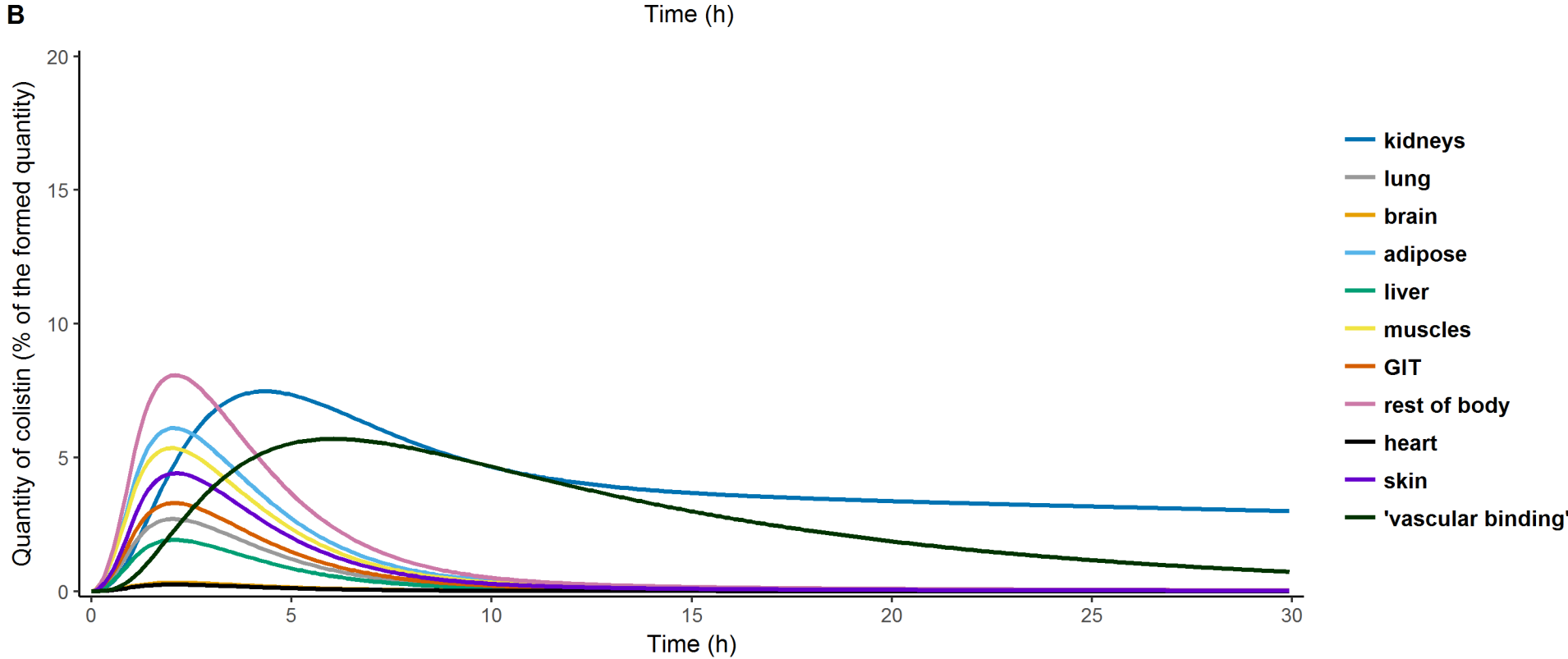
B
Quantity of colistin (% of the formed quantity)
Time (h)
kidneys
lung
brain
adipose
liver
muscles
GIT
rest of body
heart
skin
'vascular binding'

Fig. S6

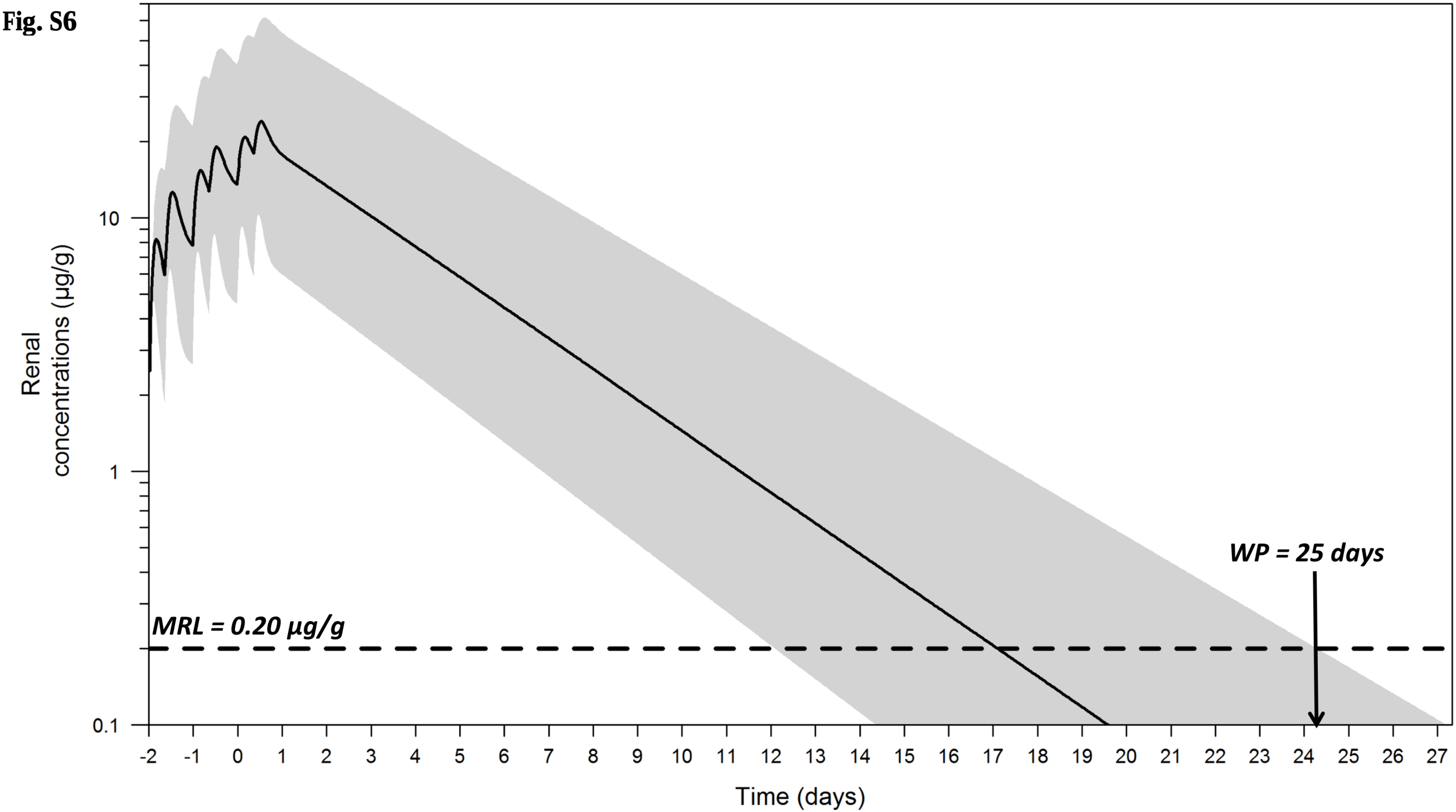
Renal concentrations (µg/g)
10
1
0.1
MRL = 0.20 µg/g
WP = 25 days
-2 -1 0 1 2 3 4 5 6 7 8 9 10 11 12 13 14 15 16 17 18 19 20 21 22 23 24 25 26 27
Time (days)

```
1
2   ;; 1. Based on: Z80
3   ;; 2. Description: LN : modèle PBPK CMS/coli
4   ;; x1. Author: user
5   ;; 3. Label:
6
7   $SIZES      PC=46 PDT=210 LVR=66 LVR2=42 LNP4=10000
8   $PROBLEM    PBPK
9   $INPUT      ID TIME CMT DV AMT RATE LLOQ UVOL EVID MDV WT OCC=DROP L2
10              STU=DROP
11  $DATA      dataset.csv IGNORE=#
12  $SUBROUTINE ADVAN14 TOL=6
13  $MODEL      COMP=(Aven1) ; venous blood (CMS)
14              COMP=(Aart1) ; arterial blood (CMS)
15              COMP=(Alun1) ; lung (CMS)
16              COMP=(Abra1) ; brain (CMS)
17              COMP=(Ahrt1) ; heart  (CMS)
18              COMP=(Amus1) ; muscle (CMS)
19              COMP=(Askn1) ; skin (CMS)
20              COMP=(Aadi1) ; adipose (CMS)
21              COMP=(Ahep1) ; liver   (CMS)
22              COMP=(Agio1) ; gut  (CMS)
23              COMP=(Akidmix1) ; kidney vascular compartment (CMS)
24              COMP=(Atub1) ; Kidney tubules (CMS)
25          COMP=(AkidEV1) ; kidney extra-vascular compartment (CMS)
26              COMP=(Akidcel1) ; kidney (intra)cellular compartment (CMS)
27          COMP=(Avessie1) ; bladder CMS
28          COMP=(Aur1) ;urine (CMS)
29              COMP=(Ares1) ;rest of body (CMS)
30          COMP=(depCMS) ; IM depot compartment (CMS)
31
32              COMP=(Aven2) ; venous blood (colistin)
33              COMP=(Aart2) ; arterial blood  (colistin)
34              COMP=(Abra2) ; brain  (colistin)
35              COMP=(Alun2) ; lung  (colistin)
36              COMP=(Ahrt2) ; heart   (colistin))
37              COMP=(Amus2) ; muscle  (colistin)
38              COMP=(Askn2) ; skin  (colistin)
39              COMP=(Aadi2) ; adipose (colistin)
40              COMP=(Ahep2) ; liver   (colistin)
41              COMP=(Agio2) ; gut   (colistin)
42              COMP=(Akidmix2) ; kidney  vascular(colistin)
43              COMP=(Atub2) ; Kidney tubule (colistin)
44              COMP=(AkidEV2) ; kidney extra-vascular compartment (colistin)
45              COMP=(Akidcel2) ; kidney (intra)cellular compartment (colistin)
46              COMP=(Akideep2) ; kidney binding compartment (colistin)
47          COMP=(Avessie2) ; bladder (colistin)
48              COMP=(Aur2) ; urine((colistin)
49          COMP=(Ares2) ; rest of body  (colistin)
50              COMP=(depColi) ;IM depot compartment (colistin))
51              COMP=(AdeepV2) ; colistin vein deep compartment
52              COMP=(AdeepA2) ; colistin artery deep compartment
53
54             COMP=(Elimccol) ; colistin elimination by metabolism (for mass balance)
55
56  $PK
57  ;; ------------------------------  Parameters ------------------------------- ;;
58
59
60  TVKHYD = THETA(1)
61  MU_1 = LOG(TVKHYD)      ;
62  KHYD = EXP(MU_1+ETA(1))     ;; hydrolysis constant of CMS into colistin
63
64  TVKNR  = THETA(2)
65  MU_2 = LOG(TVKNR)      ;
66  KNR = EXP(MU_2+ETA(2))      ;  degradation constant of colistin
67
68  TVfu_cms  = THETA(3)
69  MU_3 = LOG(TVfu_cms);
70  fu_cms = EXP(MU_3+ETA(3))    ; Unbound fraction CMS ; NOT ESTIMATED
71
72
73  TVfu_coli = THETA(4)
```

```
MU_4 = LOG(TVfu_coli)
fu_coli = EXP(MU_4+ETA(4))    ; Unbound fraction colistin  ; NOT ESTIMATED

TVKres2 = THETA(5)
MU_5 = LOG(TVKres2)      ;
Kres2 = EXP(MU_5+ETA(5))        ;    Kp of rest of body  (colistin)  ; NOT
ESTIMATED

TVka1  = THETA(6)
MU_6 = LOG(TVka1)
ka1 = EXP(MU_6+ETA(6))          ; Absorption constant of CMS for intra-muscular route

TVka2  = THETA(7)
MU_7 = LOG(TVka2)       ;
ka2 = EXP(MU_7+ETA(7)) ;         ; Absorption constant of colistin for
intra-muscular route


TVKNRcel = THETA(8)
MU_8 = LOG(TVKNRcel)      ;
KNRcel = EXP(MU_8+ETA(8))       ;   ; NOT USED

TVKmix1= THETA(9)
MU_9 = LOG(TVKmix1)       ;
Kmix1 = EXP(MU_9+ETA(9))        ;    Kp of CMS compartments (common for all
compartments)

TVkb2 = THETA(10)
MU_10 = LOG(TVkb2)      ;
kb2 = EXP(MU_10+ETA(10))         ;    "Binding" constant of colistin in vascular
compartments

TVkb2_out = THETA(11)
MU_11 = LOG(TVkb2_out)       ;
kb2_out = EXP(MU_11+ETA(11))     ;  "Unbinding" constant of colistin in vascular
compartments


TVk_on2= THETA(12)
MU_12 = LOG(TVk_on2)       ;
k_on2 = EXP(MU_12+ETA(12))      ;   "Binding" constant of colistin in kidney
intracellular compartments


TVk_off2 = THETA(13)
MU_13 = LOG(TVk_off2)       ;
k_off2 = EXP(MU_13+ETA(13))     ;   "Unbinding" constant of colistin in kidney
intracellular compartments


TVCLreab2= THETA(14)
MU_14 = LOG(TVCLreab2)       ;
CLreab2 = EXP(MU_14+ETA(14))    ;    Reabsorption of colistin tubular lumen into
intracellular compartment  ; NOT ESTIMATED


TVKCLsec1= THETA(15)
MU_15 = LOG(TVKCLsec1)       ;
CLsec1 = EXP(MU_15+ETA(15))     ;   Tubular CMS secretion from kidney vascular space
to tubular lumen









;; ------------------------- Tissue volumes (L) -------------------------- ;;


Vart = (2.65/100) *WT              ;; Arterial volume (L);
```

```
Vven = (5.3/100) * WT              ;; Venous volume (L);
Vlun = (2.7/100) * WT               ; Lung volume (L);
Vbra = (0.34/100)* WT               ; Brain volume (L);
Vhrt = (0.62/100)* WT               ; Heart volume (L);
Vmus = (37.8/100)*WT                ;; Muscle volume (L)
Vskn = (7.7/100)*WT                  ;; Skin volume (L);
Vadi = (17.7/100) *WT              ;; Adipose volume (L);
Vhep = (2.7/100)* WT                ; Liver volume (L);
Vgio = (6.18/100)*WT                ;; GIO volume stomach+Small Intestine+colon (L);
Vkid = (0.48/100) * WT              ; Kidney volume (L);
Vkidmix = (6.7/100) * Vkid          ; Vascular fraction of Kidney
VkidEV = (11.8/100) * Vkid          ; extra-Vascular fraction of Kidney
Vtub = (20/100)*Vkid                ; Tubulear fraction of Kidney
Vvessie = 0.01*WT                   ; Bladder volume
Vkidcel = Vkid- (Vkidmix + VkidEV+Vtub)  ; Cellular fraction of Kidney

Vres = WT - (Vart + Vven + Vlun + Vbra+ Vhrt + Vskn + Vmus + Vadi + Vgio + Vhep +
Vkid+Vvessie)     ;; Rest of body volume

Vtot = WT                           ; Total Volume


;; -------------------------- Blood flows (L/H) ------------------------ ;;
deb = 8.5                            ;  cardiac output (L/h/kg)
Ht = 0.35                           ; Pig hematocrit
CO = deb * WT * (1-Ht)               ; Total plasmatic flow   (L/h)

GFR = 0.074 * WT                   ; Glomerular filtration rate (L/h)


Qbra = (2.05/100) * CO              ;; Brain plasmatic flow (L/h)
Qhrt = (3.67/100) *CO                ;; Heart plasmatic flow (L/h)
Qskn = (5/100) *CO                  ; ; Skin plasmatic flow (L/h)
Qmus =  (20/100)*CO                   ;; Muscle plasmatic flow(L/h)
Qadi = (16.7/100)*CO                 ;; Adipose plasmatic flow (L/h)
Qgio = (21.5/100)*CO                   ;; GIO plasmatic flow (L/h)
QhepArt =  (5.1/100)*CO               ;; Hepatic arterial plasmatic flow (L/h)
QhepT= QhepArt + Qgio             ;; Total hepatic plasmatic flow (L/h)
Qkid = (13.45/100)*CO                ;; Kidney plasmatic flow (L/h)
Qtub = 0.67*GFR                      ;; Tubular flow in kidney (L/h)
Quri = 0.0022 * WT                  ; urinary flow, experimental data  (L/h)

SUMQ = Qmus + Qkid + Qhrt + QhepT + Qbra + Qskn + Qadi
Qres =  CO - SUMQ                                ;rest of body plasmatic flow (L/h)

Qart = CO                                             ;; Artery plasmatic flow
Qlun = CO                                            ;; Lung plasmatic flow
Qven = CO                                            ; Vein plasmatic flow


;; -------------------------- Partition Coefficients -------------------------- ;;

;------Kp CMS----;

; estimated

;-------Kp Colistin--------;

Klun2 = 0.73 * EXP(ETA(16))         ; Lung Kp (experimentally determined)
Kbra2 = 0.71 * EXP(ETA(17))         ; brain Kp (experimentally determined)
Khrt2 = 0.29 * EXP(ETA(18))         ; heart Kp (experimentally determined)
Kskn2 = 0.43 * EXP(ETA(19))         ; skin Kp (experimentally determined)
Kmus2 = 0.10 * EXP(ETA(20))         ; muscles Kp (experimentally determined)
Kadi2 = 0.25 * EXP(ETA(21))         ; Adipose Kp (experimentally determined)
Kgio2 = 0.41 * EXP(ETA(22))         ; GIO Kp (experimentally determined)
Khep2 = 0.52 * EXP(ETA(23))         ; Liver Kp (experimentally determined)


$DES
;; ------------------------ Compartment concentrations ---------------------- ;;


Cven1 = A(1)/Vven       ; venous blood (CMS)
```

```
Aven1 = A(1)
Cven2 = A(2)/Vven       ; venous blood (colistine)
Aven2 = A(2)
Aur1 = A(3)             ; urine quantities (CMS)
Chrt1 = A(4)/Vhrt           ; heart  (CMS)
Clun1 = A(5)/Vlun           ; lung  (CMS)
Cgio1 = A(6)/Vgio           ; gut (CMS)
Ckidmix1 = A(7)/Vkidmix     ; kidney vascular (CMS)
Chep1 = A(8)/Vhep           ; liver  (CMS)
Cmus1 = A(9) /Vmus          ; muscle (CMS)

Chrt2 = A(10)/Vhrt          ; heart  (colistin)
Clun2 = A(11)/Vlun          ; lung  (colistin)
Cgio2 = A(12)/Vgio          ; gut (colistin)
Ckidmix2 = A(13)/Vkidmix    ; kidney vascular (colistin)
Chep2 = A(14)/Vhep          ; liver  (colistin)
Cmus2 = A(15) /Vmus         ; muscle (colistin)

Cart1 = A(16)/Vart      ; arterial blood (CMS)
Aart1 = A(16)
Cbra1 = A(17)/Vbra      ; brain (CMS)
Cskn1 = A(18)/Vskn      ; skin  (CMS)
Cadi1 = A(19)/Vadi      ; adipose (CMS)
Avessie1 = A(20)
Cvessie1 = A(20)/Vvessie ; bladder (CMS)
Ctub1 = A(21)/Vtub      ; tubules kidney (CMS)
Cres1 = A(22)/Vres          ; rest of body  (CMS)

Aart2 = A(23)
Cart2 = A(23)/Vart      ; arterial blood (colistin)
Cbra2 = A(24)/Vbra      ; brain (colistin)
Cskn2 = A(25)/Vskn          ; skin  (colistin)
Cadi2 = A(26)/Vadi      ; adipose (colistin)
Aur2 = A(27)            ; urine quantities (colistin)
Atub2 = A(28)
Ctub2 = A(28)/Vtub      ; tubules kidney (Colistin)
Cres2 = A(29)/Vres          ; rest of body  (colistin)
Cvessie2 = A(30)/Vvessie ; bladder (colistin)

Adep1= A(31)            ; IM depot compartment (CMS)
Adep2 = A(32)           ; IM depot compartment (colistin)

CkidEV1 = A(33)/VkidEV    ; kidney extra-vascular compartment (CMS)
Akidcel1 = A(34)
Ckidcel1 = A(34)/(Vkidcel)  ; kidney cellular compartment (CMS)

CkidEV2 = A(35)/VkidEV    ; kidney extra-vascular compartment (colistin)
Akidcel2 = A(36)
Ckidcel2 = A(36)/(Vkidcel)  ; kidney cellular compartment (colistin)
Akideep2 = A(37)            ;  kidney binding compartment (colistin)



AdeepV2 = A(38)             ;; colistin vein deep compartment
AdeepA2 = A(39)             ; colistin artery deep compartment


;; ---------------------------- Tissue clearances ---------------------------- ;;
;;;;CMS hydrolysis ;;

CLart1 = KHYD * Vart     ; artery
CLven1 = KHYD * Vven     ; vein
CLlun1 = KHYD * Vlun     ; lung
CLbra1 = KHYD * Vbra     ; brain
CLhrt1 = KHYD * Vhrt     ; heart
CLmus1 = KHYD * Vmus     ; muscles
CLskn1 = KHYD * Vskn     ; skin
CLadi1 = KHYD * Vadi     ; adipose
CLhep1 = KHYD * Vhep     ; liver
CLgio1 = KHYD * Vgio     ; GIO
CLtub1 = KHYD * Vtub     ; tubules
CLkidmix1 = KHYD * Vkidmix     ; vascular kidney
```

```
CLkidEV1 = KHYD * VkidEV     ; extra-vascular kidney
CLkidcel1 = KHYD * (Vkidcel)     ; cellular kidney
CLres1 = KHYD * Vres     ; Rest of body


;;;;;;;;;;Colistin degradation clearance ;;;;;;;;


CLart2 = KNR * Vart     ; artery
CLven2 = KNR * Vven     ; vein
CLlun2 = KNR * Vlun     ; lung
CLbra2 = KNR * Vbra     ; brain
CLhrt2 = KNR * Vhrt     ; heart
CLskn2 = KNR * Vskn     ; skin
CLmus2 = KNR * Vmus     ; muscles
CLadi2 = KNR * Vadi     ; adipose
CLgio2 = KNR * Vgio     ; GIO
CLhep2 = KNR * Vhep     ; liver
CLtub2 = KNR * Vtub     ; tubules
CLkidmix2 = KNR * Vkidmix    ; vascular kidney
CLkidEV2 = KNR * VkidEV     ; extra-vascular kidney
CLkidcel2 = KNR * (Vkidcel)     ; cellular kidney
CLres2 = KNR * Vres     ; Rest of body



;; ------------------------------ Abbreviations ------------------------------ ;;
PCMS=1631.97            ; CMS molecular weight
PCOL=1166.8             ; colistin molecular weight

RPM = PCOL/PCMS         ; ratio of molecular weights


CLRcms = fu_cms * GFR   ; Clearance of glomerular filtration (CMS)
CLRcoli= fu_coli * GFR  ; Clearance of glomerular filtration (colistin)


VENinA = (Cbra1*Qbra/Kmix1) +  (Cmus1*Qmus/Kmix1) + (Chrt1*Qhrt/Kmix1)  +
(Cskn1*Qskn/Kmix1)
VENinB =  (Cadi1*Qadi/Kmix1) + (Chep1*QhepT/Kmix1) + (CkidEV1*(Qkid))
+(Cres1*Qres/Kmix1)
VENoutA = (Qven*Cven1) + (Cven1*CLven1)

HEPinA  = (QhepArt*Cart1) + (Qgio*Cgio1/Kmix1)
HEPoutA = (QhepT*Chep1/Kmix1) + (Chep1*CLhep1)

VENinC = (Cbra2*Qbra/Kbra2) +  Cmus2*Qmus/Kmus2 + (Chrt2*Qhrt/Khrt2) +
(Cskn2*Qskn/Kskn2)
VENinD = (Cadi2*Qadi/Kadi2) + (Chep2*QhepT/Khep2) + (CkidEV2*(Qkid))
+(Cres2*Qres/Kres2) + (Cven1*CLven1)*RPM
VENoutB = (Qlun*Cven2) + (Cven2*CLven2)

HEPinB  = (Cart2*QhepArt) + (Qgio*Cgio2/Kgio2) + (Chep1*CLhep1)*RPM
HEPoutB = (QhepT*Chep2/Khep2) + CLhep2*Chep2







;; ------------------------- Differential equations ------------------------- ;;


DADT(1) =  VENinA + VENinB - VENoutA + ka1 * (Adep1)    ; venous blood  (CMS)
DADT(2) =  VENinC + VENinD - VENoutB   + ka2 * (Adep2)  - kb2*Aven2 +
kb2_out*AdeepV2   ; venous blood (colistin)

DADT(3) = Cvessie1*Quri                 ; urine (CMS)

DADT(4) =   Qhrt * (Cart1 - Chrt1/Kmix1) - Chrt1*CLhrt1         ;  heart (CMS)
DADT(5) =   Qlun * (Cven1 - Clun1/Kmix1) -  Clun1*CLlun1        ;  lung (CMS)
```

```
DADT(6) =   Qgio * (Cart1 - Cgio1/Kmix1) - Cgio1*CLgio1         ; GIO (CMS)
DADT(7) =   Qkid * (Cart1 - Ckidmix1) - Ckidmix1*CLkidmix1      ; kidney vascular
(CMS)
DADT(8) =   HEPinA - HEPoutA                                    ; liver (CMS)
DADT(9) =   Qmus * (Cart1 - Cmus1/Kmix1) - Cmus1*CLmus1         ; muscle (CMS)

DADT(10) =  Qhrt * (Cart2 - Chrt2/Khrt2) + Chrt1*(CLhrt1)*RPM - Chrt2*CLhrt2
;  heart  (colistin)
DADT(11) =  Qlun * (Cven2 - Clun2/Klun2) + Clun1*(CLlun1)*RPM  - Clun2*CLlun2
;  lung  (colistin)
DADT(12) =  Qgio * (Cart2 - Cgio2/Kgio2) + Cgio1*(CLgio1)*RPM - Cgio2*CLgio2
; GIO  (colistin)
DADT(13) =  Qkid * (Cart2 - Ckidmix2)- Ckidmix2*CLkidmix2 + Ckidmix1*CLkidmix1*RPM
; kidney  vascular (colistin)
DADT(14) =  HEPinB - HEPoutB
; liver   (colistin)
DADT(15) =  Qmus * (Cart2 - Cmus2/Kmus2) + Cmus1*(CLmus1)*RPM - Cmus2*CLmus2
; muscle  (colistin)

DADT(16) =  (Qlun*Clun1/Kmix1) - (Cart1*CLart1) - (Qart*Cart1)                  ;
arterial blood (CMS)
DADT(17) =  Qbra * (Cart1 - Cbra1/Kmix1) - Cbra1*CLbra1                         ;
brain blood (CMS)
DADT(18) =  Qskn * (Cart1 - Cskn1/Kmix1) - Cskn1*CLskn1                         ;
skin (CMS)
DADT(19) =  Qadi * (Cart1 - Cadi1/Kmix1 ) -  Cadi1*CLadi1                       ;
adipose (CMS)
DADT(20) =  Ctub1*Qtub - Cvessie1*Quri                                          ;
bladder (CMS)
DADT(21) =  Ckidmix1 * CLRcms + CLsec1*Ckidcel1- Ctub1* (Qtub) - Ctub1*CLtub1  ;
tubules (CMS)
DADT(22) =  Qres * (Cart1 - Cres1/Kmix1) - Cres1*CLres1                         ;
rest of body (CMS)



DADT(23) =  Qlun*Clun2/Klun2 + Cart1*CLart1*RPM - Qart*Cart2  - Cart2*CLart2 -
kb2*Aart2 + kb2_out*AdeepA2      ; arterial blood (colistin)
; arterial blood  colistin
DADT(24) =  Qbra * (Cart2 - Cbra2/Kbra2) + Cbra1*(CLbra1)*RPM   -
Cbra2*CLbra2              ; brain (colistin)
DADT(25) =  Qskn * (Cart2 - Cskn2/Kskn2) + Cskn1*(CLskn1)*RPM  -
Cskn2*CLskn2               ;  skin (colistin)
DADT(26) =  Qadi * (Cart2 - Cadi2/Kadi2) + Cadi1*(CLadi1)*RPM  -
Cadi2*CLadi2               ; adipose (colistin)
DADT(27) =
Cvessie2*Quri*(1/RPM)                                                           ;
urine (colistin)
DADT(28) =  Ckidmix2 * CLRcoli + Ctub1*CLtub1*RPM - Ctub2*(CLtub2+Qtub) - Ctub2
*CLreab2    ; tubules (colistin)
DADT(29) =  Qres * (Cart2  - Cres2/Kres2 ) + Cres1*(CLres1)*RPM  -
Cres2*CLres2             ; rest of body (colistin)

DADT(30) = (Ctub2*Qtub -
Cvessie2*Quri)*(1/RPM)                                          ; bladder
colistin conversion into CMS

DADT(31) = - ka1 * Adep1 - KHYD *
Adep1                                                  ; IM depot compartment (CMS)
DADT(32) = KHYD*Adep1*RPM - ka2 * Adep2 - KNR *
Adep2                                      ; IM depot compartment (colistin)

DADT(33) =  (Qkid-CLRcms)*Ckidmix1 - CkidEV1*(CLkidEV1 + CLsec1) -
CkidEV1*Qkid             ; kidney extra-vascular compartment (CMS)
DADT(34) =  CkidEV1*CLsec1 -
Ckidcel1*(CLkidcel1+CLsec1)                                ; kidney cellular
compartment (CMS)


DADT(35) =  (Qkid-CLRcoli)*Ckidmix2 - CkidEV2*(CLkidEV2) - CkidEV2*Qkid
+CkidEV1*CLkidEV1 *RPM  ; kidney extra-vascular compartment (colistin)
DADT(36) =  Ctub2 *CLreab2 - Ckidcel2*CLkidcel2 + Ckidcel1*CLkidcel1*RPM +
k_off2*Akideep2 - k_on2*Akidcel2   ; kidney cellular compartment (colistin)
```

```
DADT(37) =  k_on2*Akidcel2   -
k_off2*Akideep2                                                    ; kidney
binding compartment (colistin)


DADT(38) = kb2*(Aven2) - kb2_out*AdeepV2                                    ;
colistin vein deep compartment
DADT(39) = kb2*(Aart2) - kb2_out*AdeepA2                                    ;
colistin artery deep compartment

; ---------- Mass balance check ------------ ;

Az = Cart2*CLart2 +  (Cven2*CLven2) + Clun2*CLlun2  +Cbra2*CLbra2 + Chrt2*CLhrt2
+Cmus2*CLmus2  +Cskn2*CLskn2 + Cadi2*CLadi2
Bz = Cgio2*CLgio2  + Cres2*CLres2+ CLhep2*Chep2 + KNR*Adep2 + Ckidmix2*CLkidmix2 +
Ckidcel2*CLkidcel2 + CkidEV2*CLkidEV2 + Ctub2*CLtub2


DADT(40)= Az + Bz              ; colistin elimination by degradation

CMS = A(1) +A(3) + A(4) + A(5) + A(6) + A(7) + A(8) + A(9) + A(16)  + A(17) + A(18)
+ A(19) + A(20) + A(21)  + A(22) + A(27)+ A(30)+ A(31)  + A(33) + A(34)

COLI = A(2) + A(10) + A(11) + A(12) + A(13) + A(14) + A(15)  + A(23)+ A(24) + A(25)
+ A(26)  +A(28) + A(29)  + A(32)  + A(35)  + A(36) + A(37) + A(38) + A(39)

MB = CMS + (A(40)+ COLI)*(1/RPM)  ; mass balance



;-----------------------------------
$ERROR    (ONLY OBSERVATIONS)
;-----------------------------------

CCven1 = A(1)/Vven          ; venous blood (CMS)
CCven2 = A(2)/Vven          ; venous blood (colistin)

AAur1 = A(3)                ; urinary (CMS)
CChrt1 = A(4)/Vhrt          ; heart  (CMS)
CClun1 = A(5)/Vlun          ; lung  (CMS)
CCgio1 = A(6)/Vgio          ; gut (CMS)
CCkidmix1 = A(7)/Vkidmix    ;kidney vascular (CMS)
CCkid1 = (A(7) + A(33) + A(34) + A(21))/Vkid    ; kidney  (CMS)
CChep1 = A(8)/Vhep          ; liver  (CMS)
CCmus1 = A(9)/Vmus          ; muscle (CMS)

CChrt2 = A(10)/Vhrt         ; heart  (colistin)
CClun2 = A(11)/Vlun         ; lung  (colistin)
CCgio2 = A(12)/Vgio         ; gut (colistin)
CCkidmix2 = A(13)/Vkidmix   ;kidney vascular (colistin)
CCkid2 = (A(13)  + A(36) + A(37) + A(35) +A(28))/Vkid   ; kidney  (colistin)
CChep2 = A(14)/Vhep         ; liver  (colistin)
CCmus2 = A(15)/Vmus         ; muscle (colistin)


CCart1 = A(16)/Vart         ; arterial blood (CMS)
CCbra1 = A(17)/Vbra         ; brain (CMS)
CCskn1 = A(18)/Vskn         ; skin  (CMS)
CCadi1 = A(19)/Vadi         ; adipose (CMS)
CCvessie = A(20)/Vvessie    ; bladder  (CMS)
CCtub1 = A(21)/Vtub         ; tubules (CMS)
CCres1 = A(22)/Vres         ; rest of body  (CMS)



CCart2 = A(23)/Vart         ; arterial blood (colistin)
CCbra2 = A(24)/Vbra         ; brain (colistin)
CCskn2 = A(25)/Vskn         ; skin  (colistin)
CCadi2 = A(26)/Vadi         ; adipose (colistin)
AAur2 = A(27)               ; urine (colistin)
CCtub2 = A(28)/Vtub         ; tubules (colistin)
CCres2 = A(29)/Vres         ; rest of body  (colistin)
```

```
AAdep1 = A(31)              ; ; IM depot compartment (CMS)
AAdep2 = A(32)              ; ; IM depot compartment (colistin)


CCkidEV1 = A(33)/VkidEV    ;;kidney extra-vascular (CMS)
CCkidcel1 = A(34)/(Vkidcel) ; ; kidney cellular (CMS)


CCkidEV2 = A(35)/VkidEV    ;kidney extra-vascular (colistin)
CCkidcel2 = A(36)/(Vkidcel) ; kidney cellular (colistin)
AAkideep2 = A(37)           ;kidney binding (colistin)


AAurtot = A(3)+ A(27)       ; SUM colistin and CMS in Urine


AAdeepV2 = A(38)            ;; colistin vein deep compartment
AAdeepA2 = A(39)            ;; colistin artery deep compartment



;;----------------log transformation------------

LN_CCkid1 = LOG(CCkid1)
LN_CCkid2 = LOG(CCkid2)

LN_CCkidmix1 = LOG(CCkidmix1)
LN_CCkidmix2 = LOG(CCkidmix2)

LN_AAurtot = LOG (AAurtot)

LN_CCkidtot = LOG(CCkid1+CCkid2)    ; SUM colistin and CMS in kidney
CCkidtot = (CCkid1+CCkid2)

;;--------------------------------

AA1 = A(1)
AA2 = A(2)
AA3 = A(3)
AA4 = A(4)
AA5 = A(5)
AA6 = A(6)
AA7 = A(7)
AA8 = A(8)
AA9 = A(9)
AA10 = A(10)
AA11 = A(11)
AA12 = A(12)
AA13 = A(13)
AA14 = A(14)
AA15 = A(15)
AA16 = A(16)
AA17 = A(17)
AA18 = A(18)
AA19 = A(19)
AA20 = A(20)
AA21 = A(21)
AA22 = A(22)
AA23 = A(23)
AA24 = A(24)
AA25 = A(25)
AA26 = A(26)
AA27 = A(27)
AA28 = A(28)
AA29 = A(29)
AA30 = A(30)
AA31 = A(31)
AA31 = A(31)
AA32 = A(32)
AA33 = A(33)
AA34 = A(34)
AA35 = A(35)
AA36 = A(36)
```

```
530   AA37 = A(37)
531   AA38 = A(38)
532   AA39 = A(39)
533   AA40 = A(40)
534
535
536   IF (CCven1.LE.0) CCven1=0.00001
537   IF (CCven2.LE.0) CCven2=0.00001
538   IF (AAur1.LE.0) AAur1=0.00001
539   IF (CCkid1.LE.0) CCkid1=0.00001
540   IF (CCkid2.LE.0) CCkid2=0.00001
541
542   IF(CMT.EQ.1.AND.LLOQ.EQ.0) THEN     ; Plasma experimental data  (CMS)
543   IPRED = LOG(CCven1)
544   IRES  = DV-IPRED
545   Y = IPRED + EPS(1)
546   IWRES = IRES/EPS(1)
547   ENDIF
548
549
550   IF(CMT.EQ.2.AND.LLOQ.EQ.0) THEN     ; Plasma experimental data  (colistin)
551
552   IPRED = LOG(CCven2)
553   IRES  = DV-IPRED
554   Y = IPRED + EPS(2)
555   IWRES = IRES/EPS(2)
556   ENDIF
557
558   IF(CMT.EQ.3) THEN                    ; Urine experimental data  (CMS+Colistin)
559   IPRED = LOG(AAurtot)
560   IRES  = DV-IPRED
561   Y = IPRED + EPS(5)
562   IWRES = IRES/EPS(5)
563   ENDIF
564
565   IF(CMT.EQ.7.AND.LLOQ.EQ.0) THEN     ; Kidney experimental data  (CMS+Colistin)
566   IPRED = LOG(0.8*(CCkid1+CCkid2))           ; only kidney cortex concentrations
      equal to 80 % of total kidney
567   IRES  = DV-IPRED
568   Y = IPRED + EPS(3)
569   IWRES = IRES/EPS(3)
570   ENDIF
571
572
573
574   IF(CMT.EQ.4.AND.LLOQ.EQ.0) THEN                ; Heart tissue experimental data,
      for Kp calculation  (CMS)
575   IPRED = LOG(CChrt1)
576   IRES  = DV-IPRED
577   Y = IPRED + EPS(4)
578   IWRES = IRES/EPS(4)
579   ENDIF
580
581   IF(CMT.EQ.5.AND.LLOQ.EQ.0) THEN                ; Lung tissue experimental data, for
      Kp calculation  (CMS)
582   IPRED = LOG(CClun1)
583   IRES  = DV-IPRED
584   Y = IPRED + EPS(4)
585   IWRES = IRES/EPS(4)
586   ENDIF
587
588
589   IF(CMT.EQ.6.AND.LLOQ.EQ.0) THEN                ; GIO tissue experimental data, for
      Kp calculation  (CMS)
590   IPRED = LOG(CCgio1)
591   IRES  = DV-IPRED
592   Y = IPRED + EPS(4)
593   IWRES = IRES/EPS(4)
594   ENDIF
595
596   IF(CMT.EQ.8.AND.LLOQ.EQ.0) THEN             ; Liver tissue experimental data, for Kp
      calculation  (CMS)
597   IPRED = LOG(CChep1)
```

```
IRES  = DV-IPRED
Y = IPRED + EPS(4)
IWRES = IRES/EPS(4)
ENDIF

IF(CMT.EQ.9.AND.LLOQ.EQ.0) THEN            ; Muscles tissue experimental data, for Kp calculation  (CMS)
IPRED = LOG(CCmus1)
IRES  = DV-IPRED
Y = IPRED + EPS(4)
IWRES = IRES/EPS(4)
ENDIF

IF(CMT.EQ.17.AND.LLOQ.EQ.0) THEN           ; Brain tissue experimental data, for Kp calculation  (CMS)
IPRED = LOG(CCbra1)
IRES  = DV-IPRED
Y = IPRED + EPS(4)
IWRES = IRES/EPS(4)
ENDIF

IF(CMT.EQ.18.AND.LLOQ.EQ.0) THEN           ; Skin tissue experimental data, for Kp calculation  (CMS)
IPRED = LOG(CCskn1)
IRES  = DV-IPRED
Y = IPRED + EPS(4)
IWRES = IRES/EPS(4)
ENDIF

IF(CMT.EQ.19.AND.LLOQ.EQ.0) THEN           ; Adipose tissue experimental data, for Kp calculation  (CMS)
IPRED = LOG(CCadi1)
IRES  = DV-IPRED
Y = IPRED + EPS(4)
IWRES = IRES/EPS(4)
ENDIF



;;;;;;;;;;;;;; DATA BLOQ ;;;;;;;;;;;;

IF (CMT.EQ.1.AND.LLOQ.EQ.1) THEN
F_FLAG=1                   ; what is fitted to Y is a probability
LOQ=LOG(0.15)              ; LOQ of CMS in plasma
IPRED = LOG(CCven1)
IRES  = DV-IPRED
W =  SIGMA(1,1)
DUM=(LOQ-IPRED)/(W+0.0001)
CUMD=PHI(DUM)              ; PHI = cumulative density function
Y = CUMD
ENDIF

IF (CMT.EQ.2.AND.LLOQ.EQ.1) THEN
F_FLAG=1                   ; what is fitted to Y is a probability
LOQ=LOG(0.02)               ; LOQ of colistin in plasma
IPRED = LOG(CCven2)
IRES  = DV-IPRED
W =  SIGMA(2,2)
DUM=(LOQ-IPRED)/(W+0.0001)
CUMD=PHI(DUM)              ; PHI = cumulative density function
Y = CUMD
ENDIF

IF (CMT.EQ.7.AND.LLOQ.EQ.1) THEN
F_FLAG=1 ;                what is fitted to Y is a probability
LOQ=LOG(1)                ; LOQ of kidney for CMS and colistin
IPRED = LOG(0.8*(CCkid1+CCkid2))
IRES  = DV-IPRED
W = SIGMA(3,3)
DUM=(LOQ-IPRED)/(W+0.0001)
CUMD=PHI(DUM)             ; PHI = cumulative density function
Y = CUMD
ENDIF
```

```
667
668
669
670   IF (CMT.EQ.4.AND.LLOQ.EQ.1) THEN
671   F_FLAG=1                ; what is fitted to Y is a probability
672   LOQ=LOG(1)              ; LOQ of tissue for CMS
673   IPRED = LOG(CChrt1)
674   IRES  = DV-IPRED
675   W =  SIGMA(4,4)
676   DUM=(LOQ-IPRED)/(W+0.0001)
677   CUMD=PHI(DUM)           ; PHI = cumulative density function
678   Y = CUMD
679   ENDIF
680
681   IF (CMT.EQ.5.AND.LLOQ.EQ.1) THEN
682   F_FLAG=1                ; what is fitted to Y is a probability
683   LOQ=LOG(1)              ; LOQ of tissue for CMS
684   IPRED = LOG(CClun1)
685   IRES  = DV-IPRED
686   W =  SIGMA(4,4)
687   DUM=(LOQ-IPRED)/(W+0.0001)
688   CUMD=PHI(DUM)           ; PHI = cumulative density function
689   Y = CUMD
690   ENDIF
691
692   IF (CMT.EQ.6.AND.LLOQ.EQ.1) THEN
693   F_FLAG=1                ; what is fitted to Y is a probability
694   LOQ=LOG(1)              ; LOQ of tissue for CMS
695   IPRED = LOG(CCgio1)
696   IRES  = DV-IPRED
697   W =  SIGMA(4,4)
698   DUM=(LOQ-IPRED)/(W+0.0001)
699   CUMD=PHI(DUM)           ; PHI = cumulative density function
700   Y = CUMD
701   ENDIF
702
703   IF (CMT.EQ.8.AND.LLOQ.EQ.1) THEN
704   F_FLAG=1                ; what is fitted to Y is a probability
705   LOQ=LOG(1)              ; LOQ of tissue for CMS
706   IPRED = LOG(CChep1)
707   IRES  = DV-IPRED
708   W =  SIGMA(4,4)
709   DUM=(LOQ-IPRED)/(W+0.0001)
710   CUMD=PHI(DUM)           ; PHI = cumulative density function
711   Y = CUMD
712   ENDIF
713
714   IF (CMT.EQ.9.AND.LLOQ.EQ.1) THEN
715   F_FLAG=1                ; what is fitted to Y is a probability
716   LOQ=LOG(1)              ; LOQ of tissue for CMS
717   IPRED = LOG(CCmus1)
718   IRES  = DV-IPRED
719   W =  SIGMA(4,4)
720   DUM=(LOQ-IPRED)/(W+0.0001)
721   CUMD=PHI(DUM)           ; PHI = cumulative density function
722   Y = CUMD
723   ENDIF
724
725   IF (CMT.EQ.17.AND.LLOQ.EQ.1) THEN
726   F_FLAG=1                ; what is fitted to Y is a probability
727   LOQ=LOG(1)              ; LOQ of tissue for CMS
728   IPRED = LOG(CCbra1)
729   IRES  = DV-IPRED
730   W =  SIGMA(4,4)
731   DUM=(LOQ-IPRED)/(W+0.0001)
732   CUMD=PHI(DUM)           ; PHI = cumulative density function
733   Y = CUMD
734   ENDIF
735
736   IF (CMT.EQ.18.AND.LLOQ.EQ.1) THEN
737   F_FLAG=1                ; what is fitted to Y is a probability
738   LOQ=LOG(1)              ; LOQ of tissue for CMS
739   IPRED = LOG(CCskn1)
```

```
IRES  = DV-IPRED
W =  SIGMA(4,4)
DUM=(LOQ-IPRED)/(W+0.0001)
CUMD=PHI(DUM)           ; PHI = cumulative density function
Y = CUMD
ENDIF

IF (CMT.EQ.19.AND.LLOQ.EQ.1) THEN
F_FLAG=1                ; what is fitted to Y is a probability
LOQ=LOG(1)              ; LOQ of tissue for CMS
IPRED = LOG(CCadi1)
IRES  = DV-IPRED
W =  SIGMA(4,4)
DUM=(LOQ-IPRED)/(W+0.0001)
CUMD=PHI(DUM)           ; PHI = cumulative density function
Y = CUMD
ENDIF

;;--------------------------------

$THETA
 (0.01,0.283,10)            ; hydrolysis constant of CMS into colistin
 (0.01,0.416,10)            ; degradation constant of colistin
 0.37 FIX                   ; Unbound fraction CMS ; NOT ESTIMATED
 0.4 FIX                    ; Unbound fraction colistin ; NOT ESTIMATED
 0.4 FIX                    ; Kp of rest of body  (colistin)  ; NOT ESTIMATED
 (average of Kps of colistin)
 (0.1,1.96,15)              ; Absorption constant of CMS for intra-muscular route
 (0.1,3.35,10)              ; Absorption constant of colistin for intra-muscular route
  0 FIX                        ; NOT USED
 (0.01,0.216,2)             ; Kp of CMS compartments (common for all compartments)
 (0,0.24,15)                ; "Binding" constant of colistin in vascular compartments
 (0,0.12,5)                 ; "Unbinding" constant of colistin in vascular
 compartments
 (0.01,0.0915,5)            ; "Binding" constant of colistin in kidney intracellular
 compartments
 (0,0.014,5)                ; "UnBinding" constant of colistin in kidney
 intracellular compartments
  106 FIX                   ; Reabsorption of colistin tubular lumen into
  intracellular compartment  ; NOT ESTIMATED
 (0.01,7.22,50)             ; Tubular CMS secretion from kidney vascular space to
 tubular lumen

$OMEGA  0  FIX  ; 1 ~IIV_Khyd
$OMEGA  0.0926  ; 2 ~IIV_KNR
$OMEGA  0  FIX  ; 3 ~IIV_fu cms
$OMEGA  0  FIX  ; 4~IIV_fu coli
$OMEGA  0  FIX  ; 5 ~IIV_Kres2
$OMEGA  0  FIX  ; 6 ~IIV_ka1
$OMEGA  0  FIX  ; 7 ~IIV_ka2
$OMEGA  0  FIX  ; 8 ~IIV_KNRcel
$OMEGA  0  FIX  ; 19 ~IIV_Kmix1
$OMEGA  0  FIX  ; 10 ~IIV_kb2
$OMEGA  0  FIX  ; 11 ~IIV_kbout2
$OMEGA  0  FIX  ; 14 ~IIV_k_on2
$OMEGA  0  FIX  ; 16 ~IIV_koff2
$OMEGA  0  FIX  ; 17 ~IIV_CLreabs2
$OMEGA  0.1     ; 18 ~IIV_CLsec1
$OMEGA  0  FIX  ; 21 ~IIV_Klun2
$OMEGA  0  FIX  ; 22 ~IIV_Kbra2
$OMEGA  0  FIX  ; 23 ~IIV_Khrt2
$OMEGA  0  FIX  ; 24 ~IIV_Kskn2
$OMEGA  0  FIX  ; 25 ~IIV_Kmus2
$OMEGA  0  FIX  ; 26 ~IIV_Kadi2
$OMEGA  0  FIX  ; 27 ~IIV_Kgio2
$OMEGA  0  FIX  ; 28 ~IIV_Khep2

$SIGMA  BLOCK(2)
 0.209          ; residual variability CMS plasma
 0.1 0.164      ; residual variability Coli plasma
$SIGMA  0.296   ; residual variability Kidney
$SIGMA  0.0799  ; residual variability CMS Kp
$SIGMA  0.257   ; residual variability CMS urine
```

```
807
808   $ESTIMATION PRINT=5 MAX=9999 NSIG=2 SIGL=6 METHOD=1 INTERACTION
809               LAPLACIAN POSTHOC NOABORT
810
811   $COVARIANCE UNCONDITIONAL MATRIX=R PRINT=E
812
813   $TABLE      ID TIME CMT DV PRED IPRED IRES WRES NOPRINT ONEHEADER
814               FILE=sdtabZ81
815
816   $TABLE      ID TIME CMT CCart1 CCven1 CClun1 CChrt1 CCgio1 CCkid1
817               CCkidmix1 CChep1 CCmus1 CCskn1 CCbra1 CCadi1 CCres1 CCtub1
818               CCart2 CCven2 CClun2 CChrt2 CCgio2 CCkid2 CCkidmix2 CChep2
819               CCmus2 CCskn2 CCbra2 CCadi2 CCres2 CCtub2 CCkidEV1
820               CCkidcel1 CCkidEV2 CCkidcel2 AAkideep2 MDV AAur1 AAur2
821               Adep1 Adep2 AAdeepV2 AAdeepA2 AAurtot LN_AAurtot CCkidtot
822               LN_CCkidtot DV MB IPRED LN_CCkid1 LN_CCkid2 LN_CCkidmix1
823               LN_CCkidmix2 NOPRINT ONEHEADER FILE=mytabZ82
824
825   $TABLE      ID TIME fu_cms KHYD KNR ka1 ETA1 ETA2 ETA3 ETA4 ETA5 L2
826               NOPRINT ONEHEADER NOAPPEND FILE=patabZ81
827
828   $TABLE      ID TIME AA1 AA2 AA3 AA4 AA5 AA6 AA7 AA8 AA9 AA10 AA11 AA12
829               AA13 AA14 AA15 AA16 AA17 AA18 AA19 AA20 AA21 AA22 AA23
830               AA24 AA25 AA26 AA27 AA28 AA29 AA30 AA31 AA32 AA33 AA34
831               AA35 AA36 AA37 AA38 AA39 AA40 MB NOPRINT ONEHEADER
832               FILE=mytabZ81_2
833
834   $TABLE      ID TIME CLart1 CLart2 CLven1 CLven2 CLlun1 CLlun2 CLbra1
835               CLbra2 CLhrt1 CLhrt2 CLskn1 CLskn2 CLmus1 CLmus2 CLadi1
836               CLadi2 CLgio1 CLgio2 CLhep1 CLhep2 CLtub1 CLtub2 NOPRINT
837               ONEHEADER FILE=mytabZ81_1
838
```